Injectivity Characteristics of EOR Polymers

Abstract

For applications where EOR polymer solutions are injected, we estimate injectivity losses (relative to water injectivity) if fractures are not open. We also consider the degree of fracture extension that may occur if fractures are open. Three principal EOR polymer properties are examined that affect injectivity: (1) debris in the polymer, (2) polymer rheology in porous media, and (3) polymer mechanical degradation. An improved test was developed to measure the tendency of EOR polymers to plug porous media. The new test demonstrated that plugging tendencies varied considerably among both partially hydrolyzed polyacrylamide (HPAM) and xanthan polymers.

Rheology and mechanical degradation in porous media were quantified for a xanthan and an HPAM polymer. Consistent with previous work, we confirmed that xanthan solutions show pseudoplastic behavior in porous rock that closely parallels that in a viscometer. Xanthan was remarkably resistant to mechanical degradation, with a 0.1% xanthan solution (in seawater) experiencing only a 19% viscosity loss after flow through 102-md Berea sandstone at a pressure gradient of 24,600 psi/ft.

For 0.1% HPAM in both 0.3% NaCl brine and seawater in 573-md Berea sandstone, Newtonian behavior was observed at low to moderate fluid fluxes, while pseudodilatant behavior was seen at moderate to high fluxes. No evidence of pseudoplastic behavior was seen in the porous rock, even though one solution exhibited a power-law index of 0.64 in a viscometer. For this HPAM in both brines, the onset of mechanical degradation occurred at a flux of 14 ft/d in 573-md Berea.

Considering the polymer solutions investigated, satisfactory injection of more than 0.1 *PV* in field applications could only be expected for the cleanest polymers (i.e., that do not plug before 1,000 cm^3/cm^2 throughput), without inducing fractures (or formation parts for unconsolidated sands). Even in the absence of face plugging, the viscous nature of the solutions investigated requires that injectivity must be less than one-fifth that of water if formation parting is to be avoided (unless the injectant reduces the residual oil saturation and substantially increases the relative permeability to water). Since injectivity reductions of this magnitude are often economically unacceptable, fractures or fracture-like features are expected to open and extend significantly during the course of most polymer floods. Thus, an understanding of the orientation and growth of fractures may be crucial for EOR projects where polymer solutions are injected.

Introduction

Maintaining mobility control is essential during chemical floods (polymer, surfactant, alkaline floods). Consequently, viscosification using water soluble polymers is usually needed during chemical enhanced oil recovery (EOR) projects. Unfortunately, increased injectant viscosity could substantially reduce injectivity, slow fluid throughput, and delay oil production from flooded patterns. The objectives of this paper are to estimate injectivity losses associated with injection of polymer solutions if fractures are not open and to estimate the degree of fracture extension if fractures are open. We examine the three principal EOR polymer properties that affect injectivity: (1) debris in the polymer, (2) polymer rheology in porous media, and (3) polymer mechanical degradation. Although some reports suggest that polymer solutions can reduce the residual oil saturation below values expected for extensive waterflooding (and thereby increase the relative permeability to water), this effect is beyond the scope of this paper.

Injectivity:

- Defined as injection rate divided by pressure drop from the wellbore into the formation.
- Want a high injectivity to allow rapid displacement and recovery of oil.

- Polymers are needed for mobility control for most chemical flooding projects:
- The viscous nature of polymer solutions will necessarily reduce injectivity unless the well intersects a fracture.
- Fractures can cause severe channeling and/or injection out of zone for expensive EOR fluids.

Objectives:

- Estimate injectivity losses associated with polymer solutions if fractures are not open.
- Estimate the degree of fracture extension if fractures are open.

Factors Affecting Polymer Solution Injectivity:

- Debris/microgels/undissolved polymer
- Rheology in porous media
- Mechanical degradation
- Displacement of residual oil (not considered here)

Debris Filtration When Entering a Porous Medium

During preparation of polymer solutions, ineffective polymer hydration and debris in the polymer can lead to near-wellbore plugging (Burnett 1975). This fact was highlighted during the Coalinga polymer demonstration project in the late 1970s (Peterson 1981, Duane and Dauben 1983). Concern about polymer solution injectivity led to the development of "filter tests" using membrane filters to assess plugging (API 1990, Levitt and Pope 2008). The typical filter test passed ~600 cm^3 of polymer solution through a 47-mm-diameter filter: yielding a throughput value of ~35 cm^3/cm^2. (Throughput is the volume of fluid per flow area.) A "filter ratio" was defined as the time to pass a fixed solution volume (e.g., 100 cm^3, using a fixed pressure drop) near the end of the test (e.g., after 20 cm^3/cm^2 throughput) divided by the time to pass the same solution volume near the beginning of the test (e.g., before 20 cm^3/cm^2 throughput). Unfortunately, field throughputs are much greater than the values used during these tests. For example, injecting 0.5 pore volumes (*PV*) of polymer solution into a 9-inch-diameter vertical well with an open-hole completion in a 20-acre pattern (constant formation height, 20%

porosity) would lead to a throughput around 1,130,000 cm^3/cm^2. If the well was intersected by a two-wing fracture, with each fracture wing at 50 ft long, the throughput for this case would drop to 13,300 cm^3/cm^2. These figures point out the need for a filter test with throughput values that are more representative of field operations.

We developed an improved test, using much higher polymer solution throughputs than in previous tests. Berea sandstone cores (100-600 md permeability, 21% porosity) and various filters and filter combinations were used to measure the plugging tendency versus throughput. Our new test was applied to compare many potential EOR polymers.

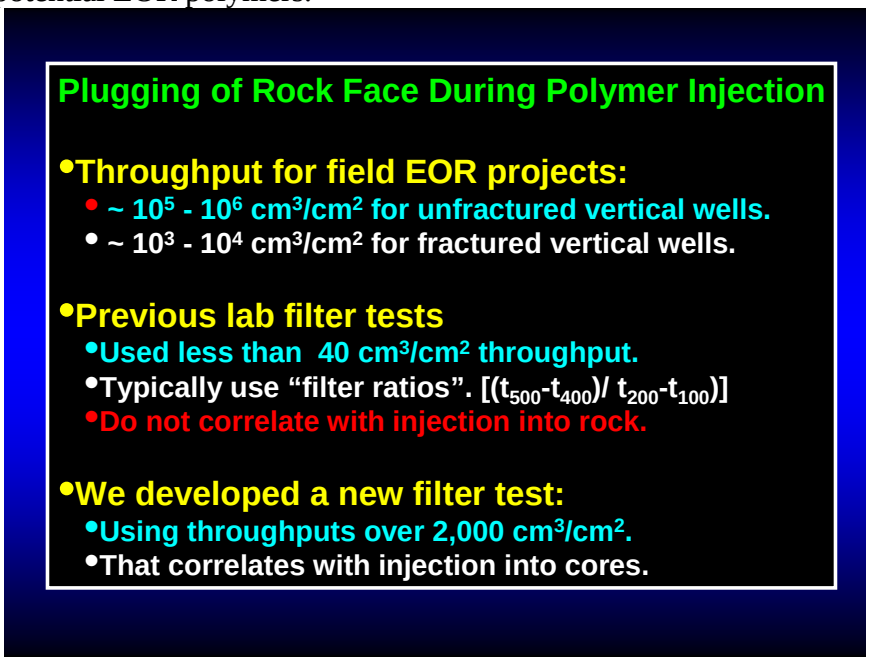

Polymers and Solutions. Although we examined many EOR polymers, our focus was on one xanthan and one partially hydrolyzed polyacrylamide (HPAM). The xanthan gum, K9D236™, Lot #6441F470C, was supplied as a white powder by CP Kelco. This polymer has a molecular weight between 2 and 2.5 million Daltons and a pyruvate content of 4.5%. Hereafter, this polymer will be called X US K K36 xanthan. SNF provided the powder-form HPAM, FLOPAAM 3830S™, Lot X1899 (stated molecular weight: 20-22 million Daltons, degree of hydrolysis: ~30%). Hereafter, this polymer will be labeled P FR S 38 HPAM. A number of other polymers were examined during the course of this work, which we labeled: X US K HV, X US K XC, X US K K70, X CH Sh F, P CH H H22, P CH H K5, and P FR S 60. These coded labels were assigned to minimize commercial implications. Labels that begin with X are xanthans, while those that begin with P are partially hydrolyzed polyacrylamides. The second set of letters codes a country, the third set codes a manufacturer, and the fourth set codes a polymer product.

Sea salt, ASTM D-1141-52, was used to make our synthetic seawater. This seawater contained 4.195% sea salt in distilled water (i.e., 4.195% total dissolved solids or TDS), including 0.13% Mg^{2+} and 0.042% Ca^{2+}. A second brine contained 2.52% TDS, with no divalent cations. Although the make-up brine was filtered (through 0.45 µm filters), no filtration occurred after polymer addition. No biocide was added, and injection began shortly after preparation of the polymer solutions.

Core Tests. During the core tests, ~27 liters of freshly prepared polymer solutions were forced through Berea sandstone cores that were ~14.5 cm long and 11.34 cm^2 in cross section. Each core had two internal pressure taps, located 2 cm from the inlet and outlet sand faces. Our cores were cast in a metal alloy, saturated with brine, and then porosity and permeability (to brine) were determined. Finally, polymer solution injection was initiated. A new core was used for each polymer and plugging test. Berea core porosities averaged 21% (ranging from 20-22%). The injection rate was 2,000 cm^3/hr or 139 ft/d flux (i.e., 139 $ft^3/ft^2/d$). This volume of fluid injection through the sand face area translated to a throughput of about 2,300 cm^3/cm^2.

Fig. 1 plots resistance factors for the three Berea core sections as a function of xanthan solution throughput (for 0.1% X US K K36 xanthan in seawater). Resistance factor is defined as brine mobility divided by polymer solution mobility. Assuming that the permeability of the core is fixed, resistance factor is the effective viscosity of the polymer solution in porous media relative to brine. Fig. 1 demonstrates that the resistance factors in the second (middle, longest) and third (last) core section were quite stable during the course of X US K K36 xanthan injection. Resistance factor averaged 3.8 in the second core section and 3.1 in the third core section. Thus, no in-depth plugging was noted within the core.

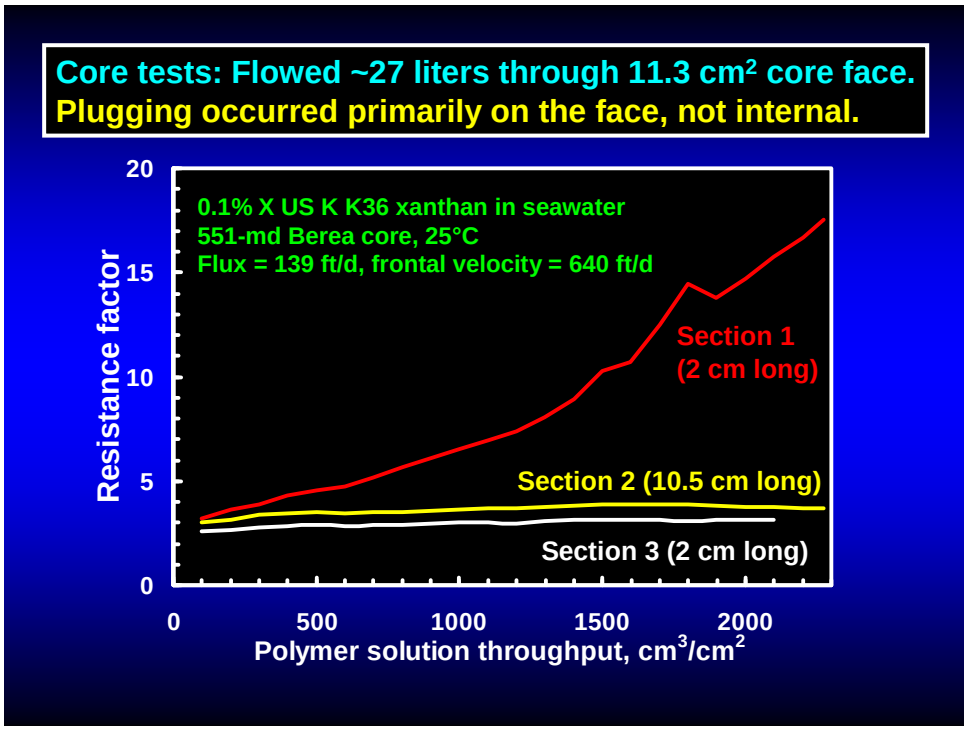

Fig. 1—Xanthan resistance factors versus throughput for the three core sections.

In the first core section, resistance factors increased from 3.2 to 17.5 over the course of injecting 2,300 cm^3/cm^2 (770 *PV*) of X US K K36 xanthan solution. Thus, some plugging of the injection sand face was noted, but the degree of plugging was mild considering the large total throughput. Fig. 2 (yellow curve) plots the data differently to appreciate this point. The *y*-axis plots filter cake resistance, l_s/k_s, expressed in cm/darcy. This term can be applied along with the Darcy equation. For example, for a filter cake that builds up at the core surface, Eq. 1 can be used.

$$q/\Delta p = [A/(\mu_w F_r)] / [L/k_m + l_s/k_s] \quad (1)$$

In this equation, q, is injection rate, Δp is the pressure difference across the core, A is core cross-sectional area, L is core length, μ_w is water viscosity, F_r is resistance factor (specifically in the second section of the core), and k_m is the original core permeability to brine.

We established filter cake resistance on 550-md Berea sandstone cores (all permeabilities given in this paper are permeability to brine) as a function of throughput for seawater solutions of 0.1% xanthan (X US K K36) and partially hydrolyzed polyacrylamide (P FR S 38). Fig. 2 summarizes these results. Face plugging by X US K K36 xanthan was quite low over the course of injecting 2,300 cm^3/cm^2 of 0.1% xanthan solution in seawater (yellow curve in Fig. 2). When injecting an equivalent throughput of 0.1% P FR S 38 HPAM, the polymer's viscoelastic (or "pseudodilatant" or "shear thickening") behavior (Jennings *et al*. 1971, Hirasaki and Pope 1974) caused the absolute level of flow resistance to be considerably higher than that for xanthan. (This effect will be discussed more in the next section.) After subtracting out this viscoelastic effect, the level of face plugging (i.e., the slope of the red curve in Fig.

2) was greater than that for X US K K36 xanthan. Nevertheless, face plugging by P FR S 38 HPAM was relatively low during this experiment. (For each of the curves in Figs. 2 and 3, a separate core was used, although the solid circles in Fig. 2 are the same data as the solid squares in Fig. 3.)

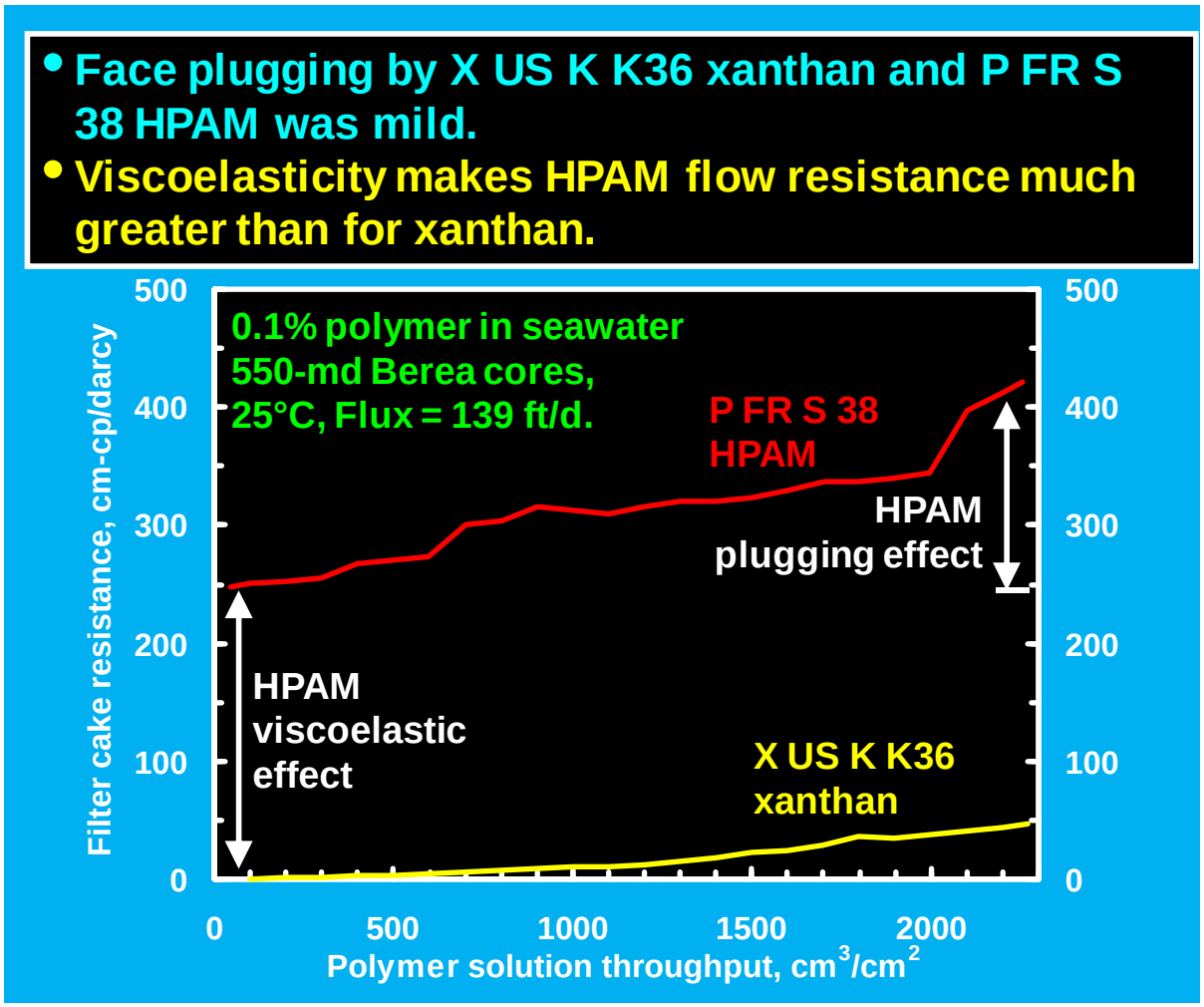

Fig. 2—Filtration results for X US K K36 xanthan and P FR S 38 HPAM in 550-md Berea cores.

For 0.1% X US K K36 xanthan in seawater, Fig. 3 shows the development of face plugging as a function of core permeability, with Berea cores ranging from 102 to 551 md. As expected, face plugging was more severe as permeability decreased. For throughput values between 1,000 and 2,000 cm^3/cm^2, the filter cake resistance was roughly seven times greater for 102-md Berea than for 191-md Berea, which in turn was about seven times greater than for 551-md Berea. Fig. 4 re-plots the data in Fig. 3, after multiplying the filter cake resistance by the factor, $(k/551)^2$, where permeability, k, is given in md. This procedure helps to normalize the three curves.

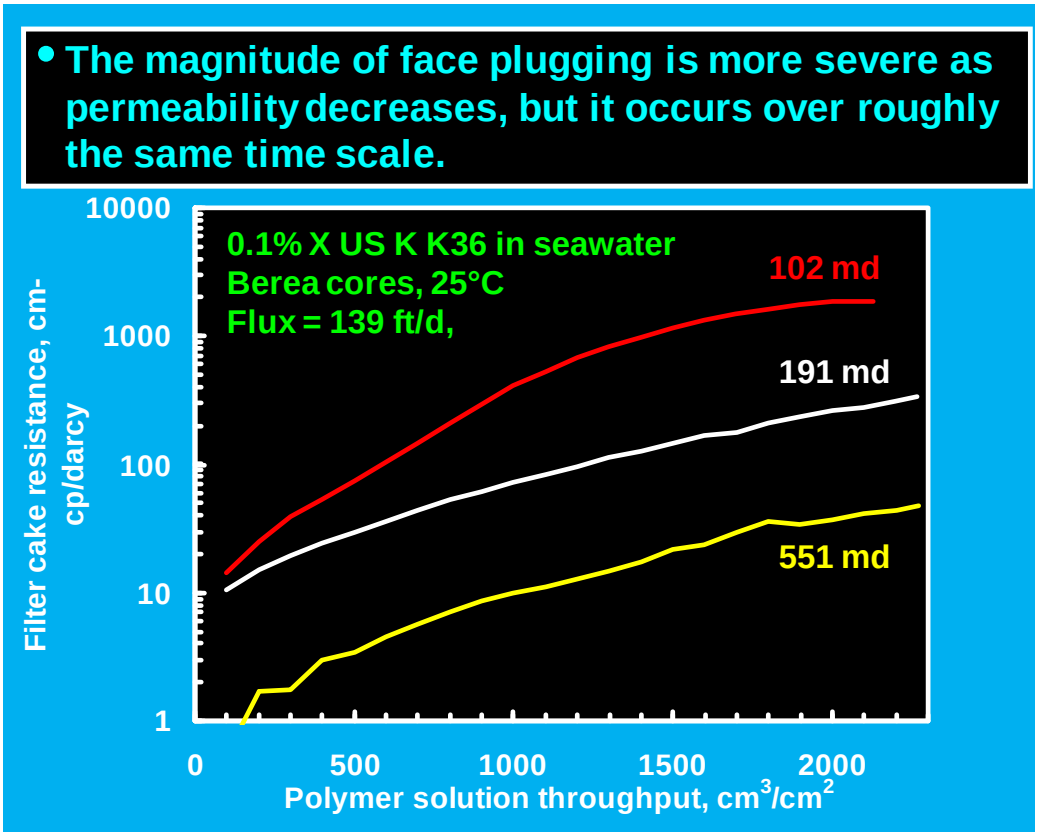

Fig. 3—Filtration results for X US K K36 xanthan Berea cores with various permeabilities.

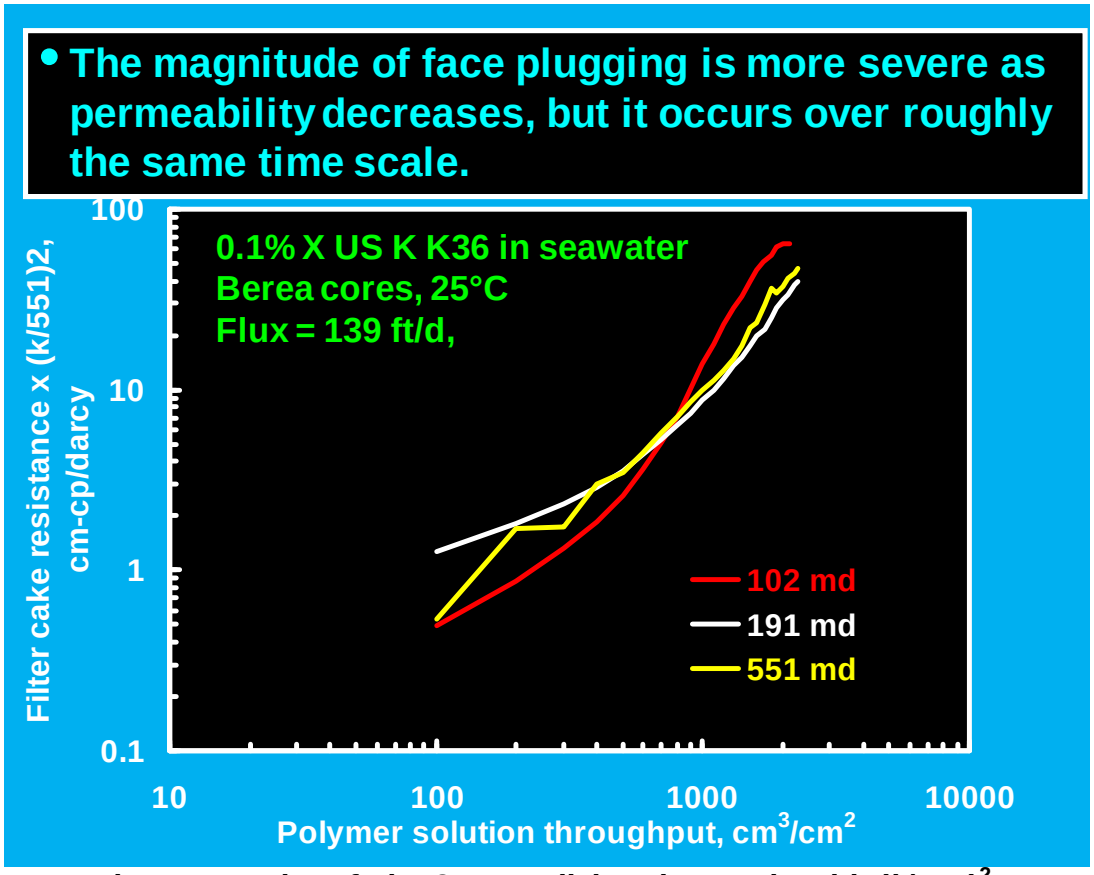

Fig. 4—Re-plot of Fig. 3 normalizing the y-axis with $(k/551)^2$.

A New Filter Test. Because tests using cores are relatively expensive and time consuming, we developed a filter test using filters that mimicked the plugging behavior seen during the core tests. After some experimentation, we identified a workable test using a Millipore AP10™ filter pad upstream of a 10 µm polycarbonate (Sterlitech Track Etch™) membrane filter (both 13 mm in diameter). Fig. 5 compares filtration results for X US K K36 xanthan (yellow curve) with results from the core test (red curve). The filter cake resistance (cm-cp/darcy) from the filtration test must be multiplied by 10 to match the cm-cp/darcy level from the 551-md Berea core result. However, the key positive point is that the plugging rate matches throughput fairly well for the core and filter comparison (white versus red curves).

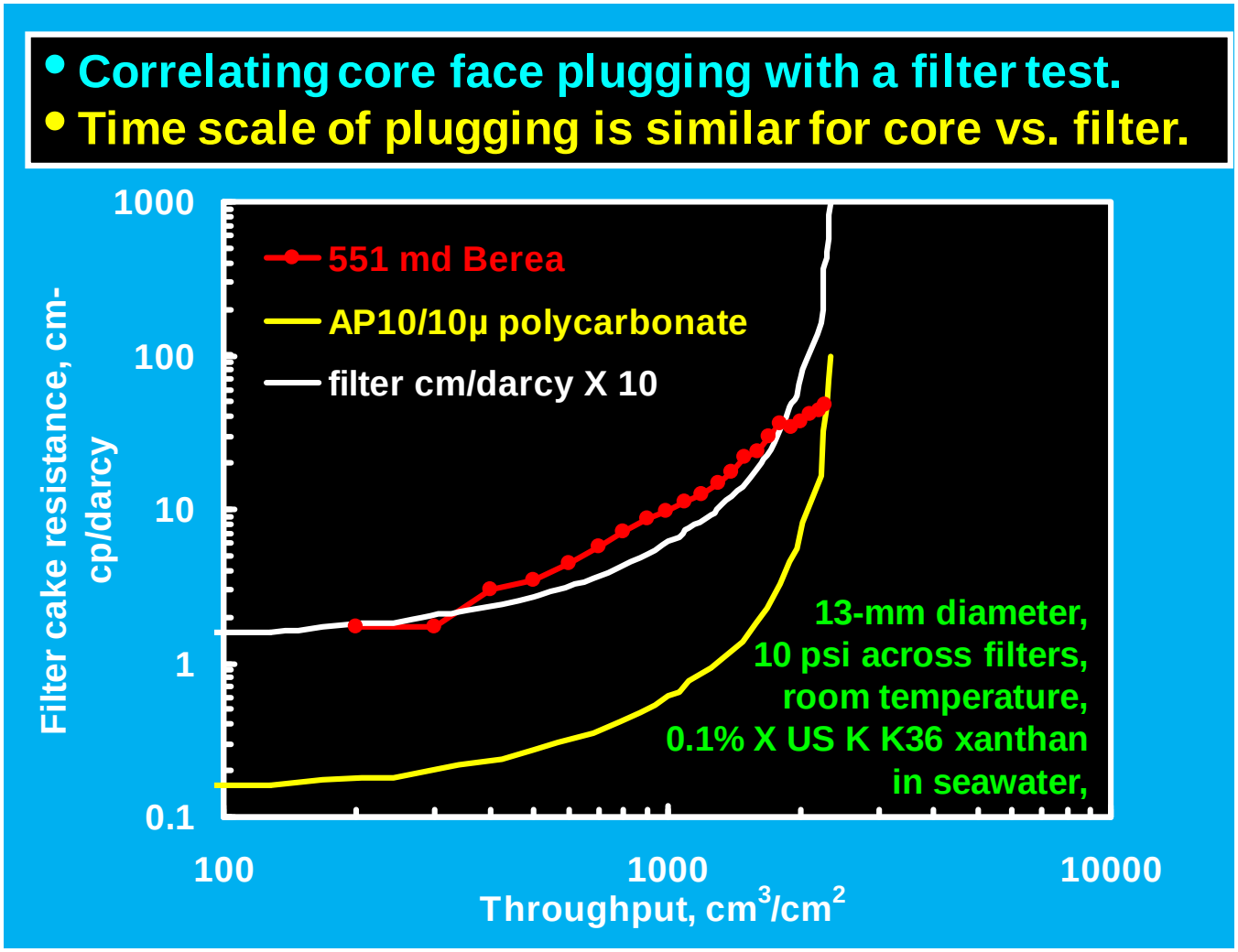

Fig. 5—Plugging trends for X US K K36 xanthan in Berea core versus in filters.

Filterability using our new test is compared for various polymers in synthetic seawater in Fig. 6 and in a 2.52% brine (with no divalent cations) in Fig. 7. (Solution viscosities at a shear rate of 7.3 s^{-1} are listed in the legends.) For non-plugging polymers, our throughput values typically exceeded 1,000 cm^3/cm^2. Of the 17 tests shown in these two figures, 12 tests exhibited filter ratios near unity—meaning that the old "filter ratio" test (defined earlier, API 1990) was not capable of distinguishing between the performances of most polymer solutions shown. Also, the relevance of results from the old test to plugging in field applications is unclear. In contrast, our new test effectively demonstrated significant differences in plugging, and (as will be shown) test results can be directly related to field applications.

Examination of Figs. 6 and 7 reveals that the filter cake resistance starts at a much higher level for HPAM polymers (yellow symbols) than for xanthan polymers (non-yellow symbols). As mentioned earlier (and as will be discussed in detail in the next section), much of this effect is attributed to viscoelasticity of HPAM (Jennings *et al.* 1971, Hirasaki and Pope 1974).

A second point from these two figures is that filterability varied considerably among both HPAM and xanthan polymers. In both brines, X US K K36 xanthan (pink circles) and 0.1% P FR S 38 HPAM (yellow circles in Fig. 6, red circles in Fig. 7) exhibited excellent filterability (no significant plugging until greater than 2,000 cm^3/cm^2), while X CH SH F xanthan (red circles in Fig. 6, blue circles in Fig. 7) and X CH H K5 HPAM (yellow squares) showed poor filterability (significant plugging with less than 100 cm^3/cm^2). Interestingly, X US K HV, X US K XC, and X US K K70 xanthans showed remarkably similar filterability (blue, green, and white circles in Fig. 6 and white circles in Fig. 7).

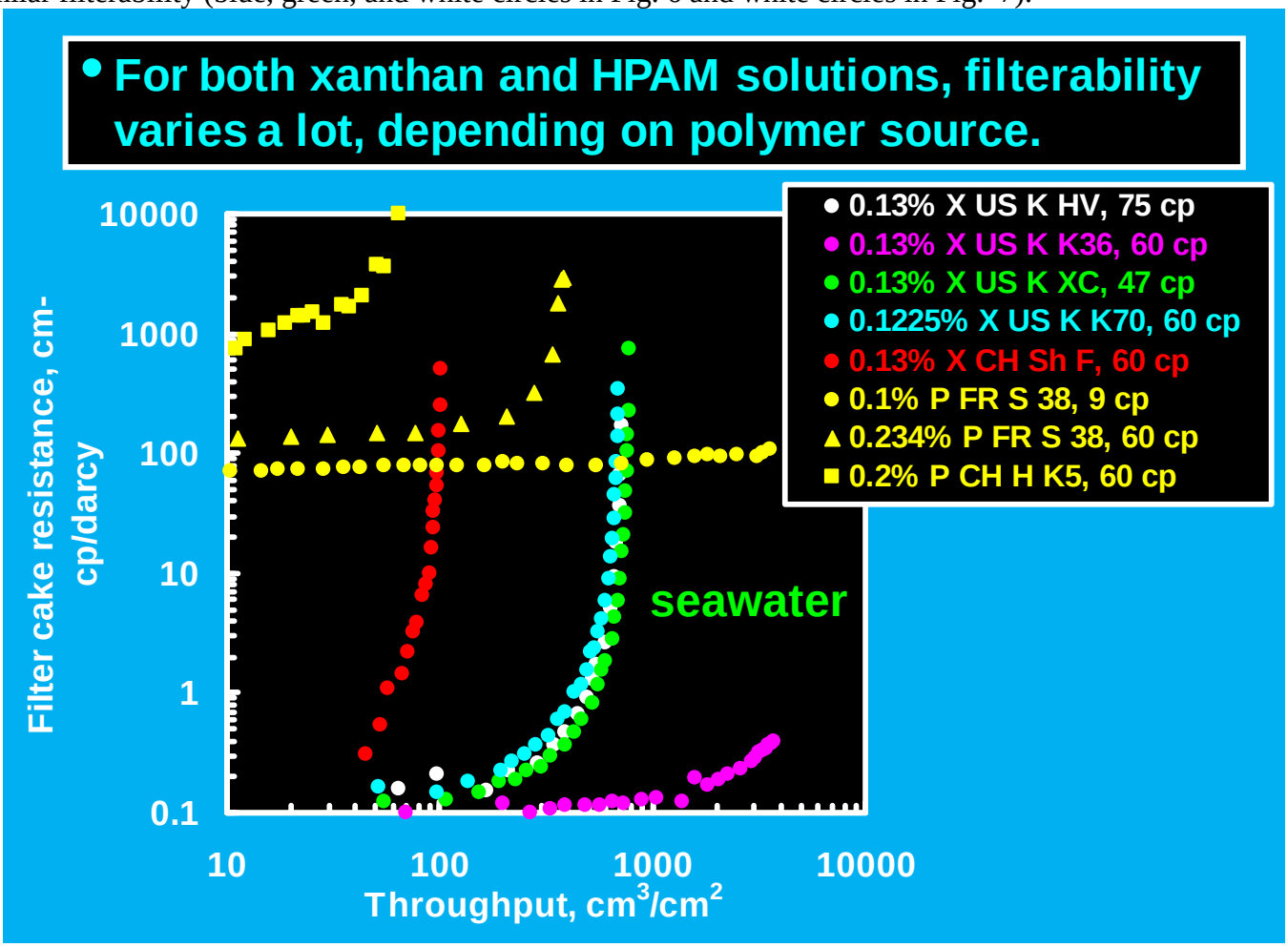

Fig. 6—Filter test results for various polymers in seawater.

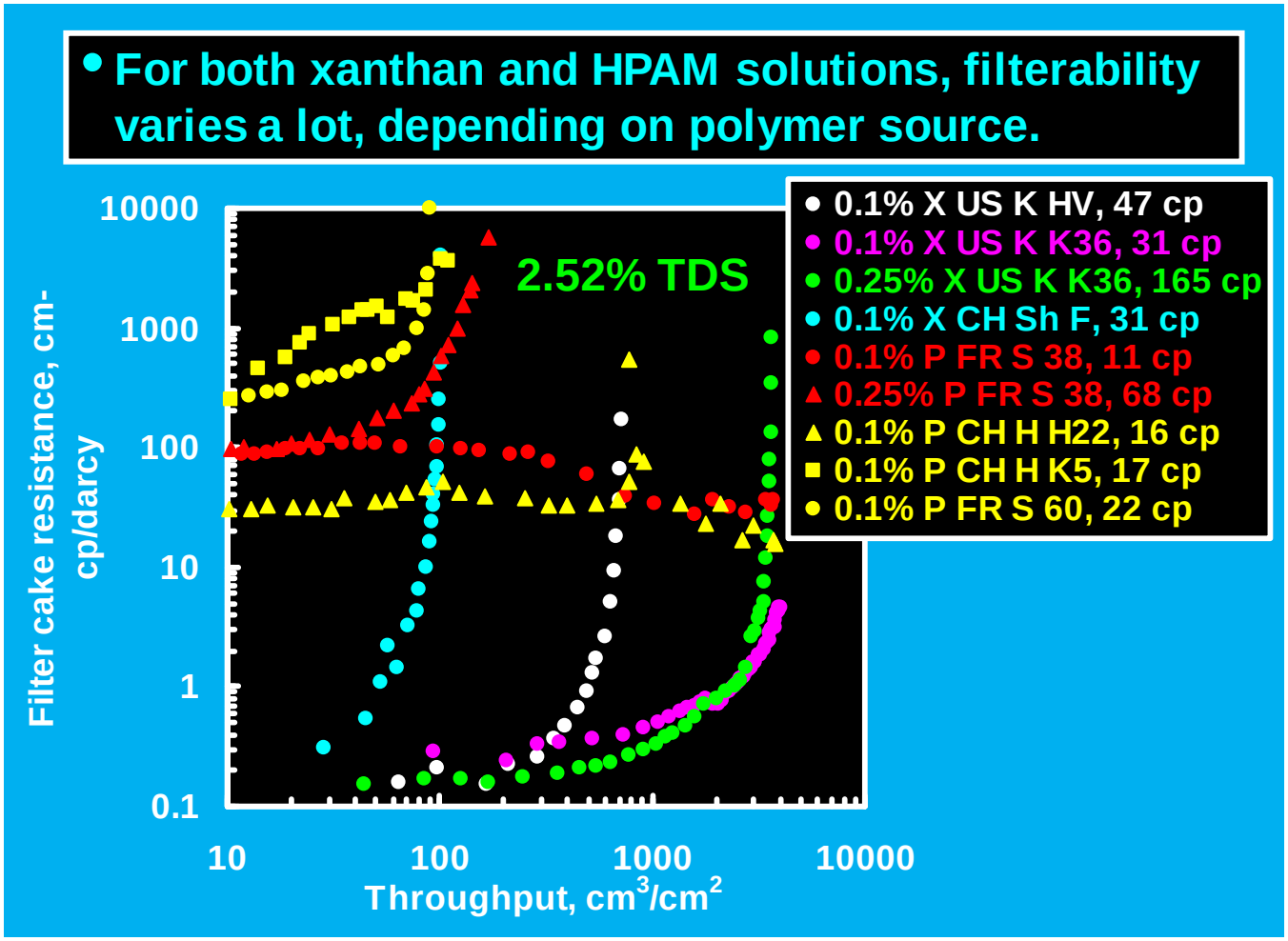

Fig. 7—Filter test results for various polymers in brine with 2.52% TDS.

For X US K K36 xanthan, filterability was virtually the same for 31-cp, 0.1% polymer (pink circles in Fig. 7) as for 165-cp, 0.25% polymer (green circles in Fig. 7). In contrast, for P FR S 38 HPAM, the filterability for 9-11-cp, 0.1% polymer (yellow circles in Fig. 6 red circles in Fig. 7) was much better than for 60-68-cp, 0.234%-0.25% polymer (yellow triangles in Fig. 6 and red triangles in Fig. 7).

Rheology in Porous Media and Mechanical Degradation

Xanthan. Rheology in porous media can have a major impact on injectivity (Seright 1983). Most EOR polymers exhibit pseudoplastic (or "shear thinning") behavior in a viscometer (Liauh and Liu 1984)—i.e., viscosity decreases with increased shear rate. Xanthan solutions are well known to provide pseudoplastic behavior in porous rock that closely parallels that in a viscometer (Burnett 1975, Chauveteau 1982, Hejri *et al*. 1988, Cannella *et al*. 1988). We demonstrate this point with X US K K36 xanthan in Fig. 8. Using a Berea sandstone core with dimensions described earlier, we injected a 0.1% xanthan solution (in seawater) using a very wide range of flux values (0.035 to 2,222 $ft^3/ft^2/d$, achieved using ISCO Model 500D and 1000D™ pumps). The xanthan resistance factor (F_r) versus flux (u, in $ft^3/ft^2/d$ or ft/d) data in Fig. 8 can be described well by Eq. 2.

$$F_r = 2.5 + 20\, u^{-0.5} \qquad (2)$$

Xanthan is known to be remarkably resistant to shear or mechanical degradation (Sorbie 1991). In Fig. 9, we plot viscosity versus shear rate for solutions of 0.1% X US K K36 xanthan (in seawater) after flow through 102-md Berea sandstone at various pressure gradients up to 24,600 psi/ft. When measured at a shear rate of 7.3 s^{-1}, the viscosity loss was only 9% using 2,480 psi/ft and 19% using 24,600 psi/ft.

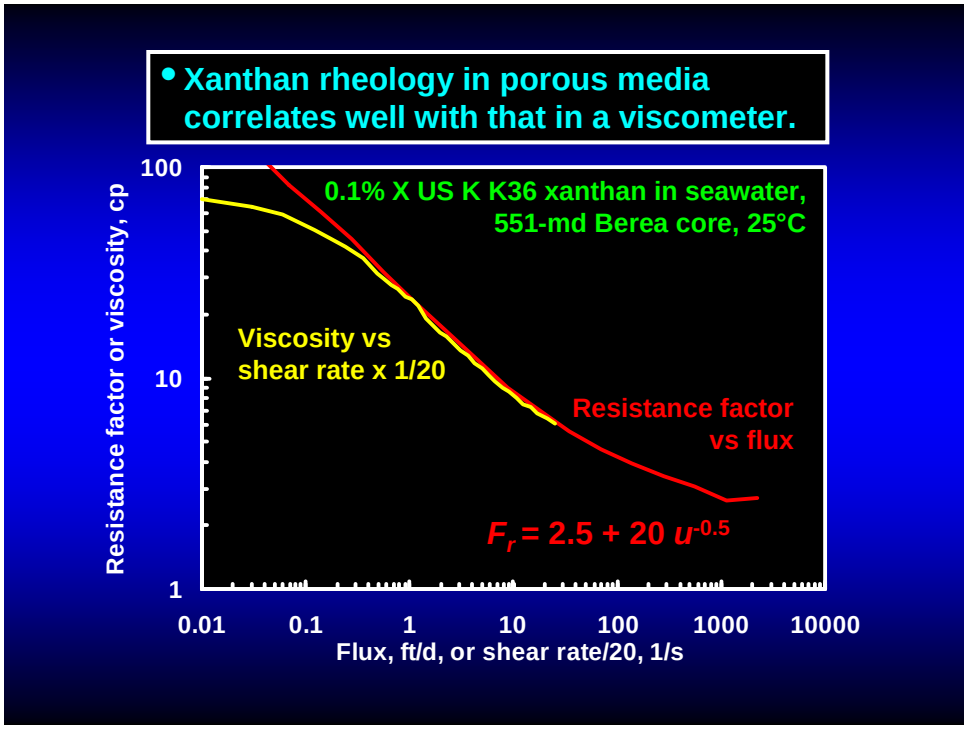

Fig. 8—Viscosity versus shear rate and resistance factor versus flux for xanthan.

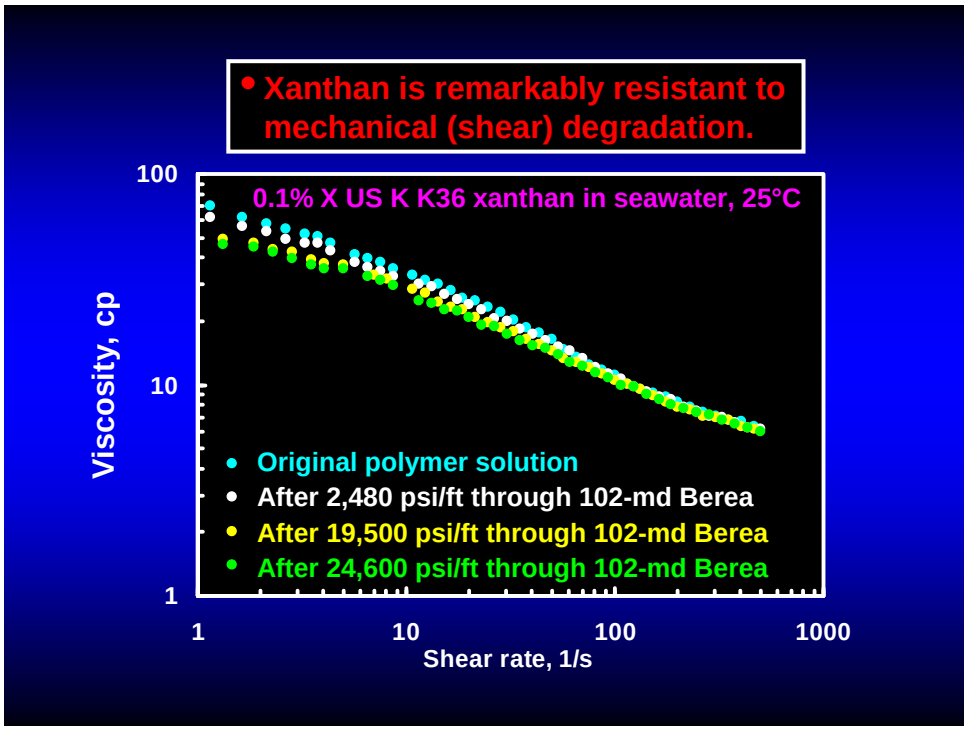

Fig. 9—Viscosity losses for xanthan after flow through 102-md Berea at high pressure gradients.

HPAM. In porous media, HPAM solutions show pseudodilatant or viscoelastic behavior—the resistance factor increases with increased flux for moderate to high fluid velocities (Pye 1964, Smith 1970, Jennings *et al*. 1971, Hirasaki and Pope 1974, Seright 1983, Masuda *et al*. 1992). HPAM solutions are also susceptible to mechanical degradation (Maerker 1975, 1976, Seright 1983). In the following figures and discussion, we demonstrate these points for solutions of 0.1% P FR S 38 HPAM in 0.3% NaCl brine and in seawater (4.195% TDS). First, consider Fig. 10, where 0.1% P FR S 38 HPAM in 0.3% NaCl brine was injected at various flux values into 573-md Berea sandstone (same core dimensions as

described earlier). When injecting fresh polymer solution at low flux (0.017 to 0.14 ft/d, red triangles in Fig. 10), resistance factors averaged 71 and showed Newtonian (flow rate independent) behavior. This resistance factor value was 87% greater than the zero-shear viscosity (38 cp) for this solution. This finding was consistent with literature reports that HPAM solutions can provide somewhat higher effective viscosities (i.e., resistance factors) in porous media than in a viscometer (Pye 1964, Smith 1970), caused by polymer retention within the rock. As flux was increased from 0.14 to 7 ft/d, resistance factors increased to 452 (again, red triangles in Fig. 10). Resistance factor versus flux from 0.017 to 7 ft/d was described reasonably well using Eq. 3 (red solid curve in Fig. 10).

$$F_r = 65 + 90\, u^{0.75} \quad (3)$$

For flux values up to 14 ft/d (pressure gradients up to 1,985 psi/ft), effluent from the core exhibited no loss of viscosity, as compared with fresh polymer solution and as measured at a shear rate of 11 s^{-1}, 25°C using a Contraves Low Shear 30™ viscometer (red triangles in Fig. 11). For higher fluid velocities, effluent viscosities decreased, with a 15% viscosity loss seen at a flux of 41 ft/d (with a pressure gradient in the core of 4,640 psi/ft). Resistance factors appeared to go through a maximum at 14-18 ft/d (red triangles in Fig. 10). The decline in resistance factor for flux values above the maximum occurred because of mechanical degradation of the polymer (Seright 1983). Above ~14 ft/d, each time the flux was raised, the polymer was mechanically degraded to a greater level, so the measured resistance factors apply to polymers with different molecular weights (Seright *et al.* 1981). If polymer effluent from 41 ft/d is re-injected at a series of lower rates (yellow triangles in Fig. 10), resistance factors showed a monotonic decrease with decreasing flux—approaching 42 at the lowest fluxes. This resistance factor value was 71% greater than the zero-shear viscosity (24.6 cp) for this solution. Resistance factor versus flux for this re-injected solution was described reasonably well using Eq. 4 (yellow dashed curve in Fig. 10).

$$F_r = 42 + 11\, u \quad (4)$$

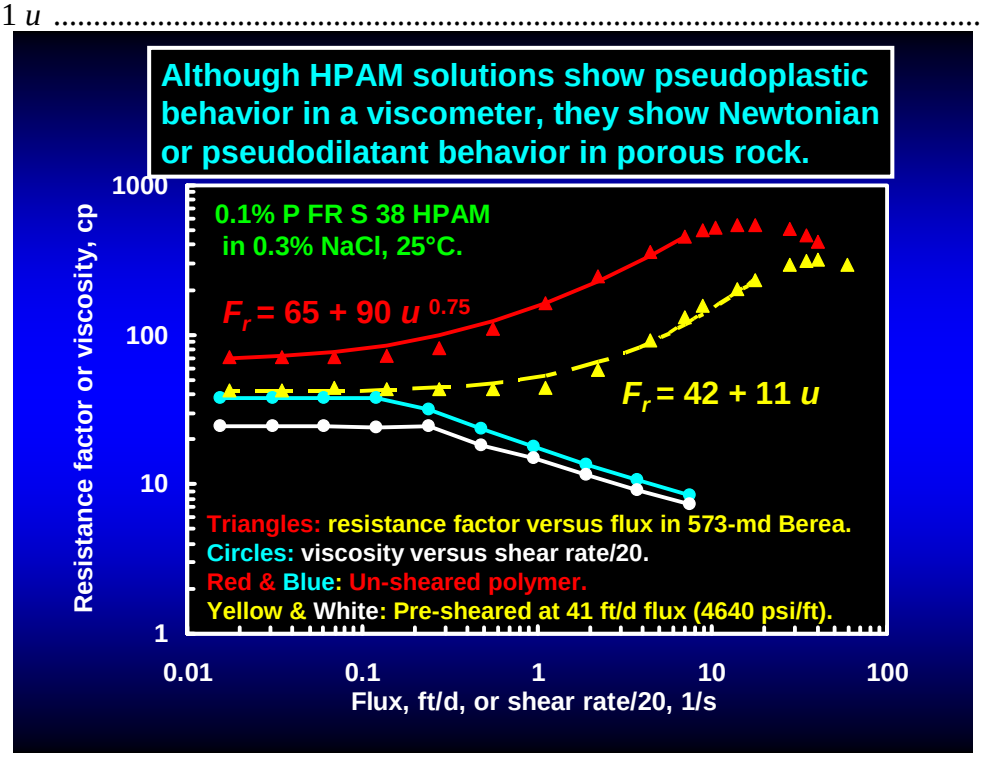

Fig. 10—Resistance factor versus flux for HPAM in 0.3% NaCl brine.

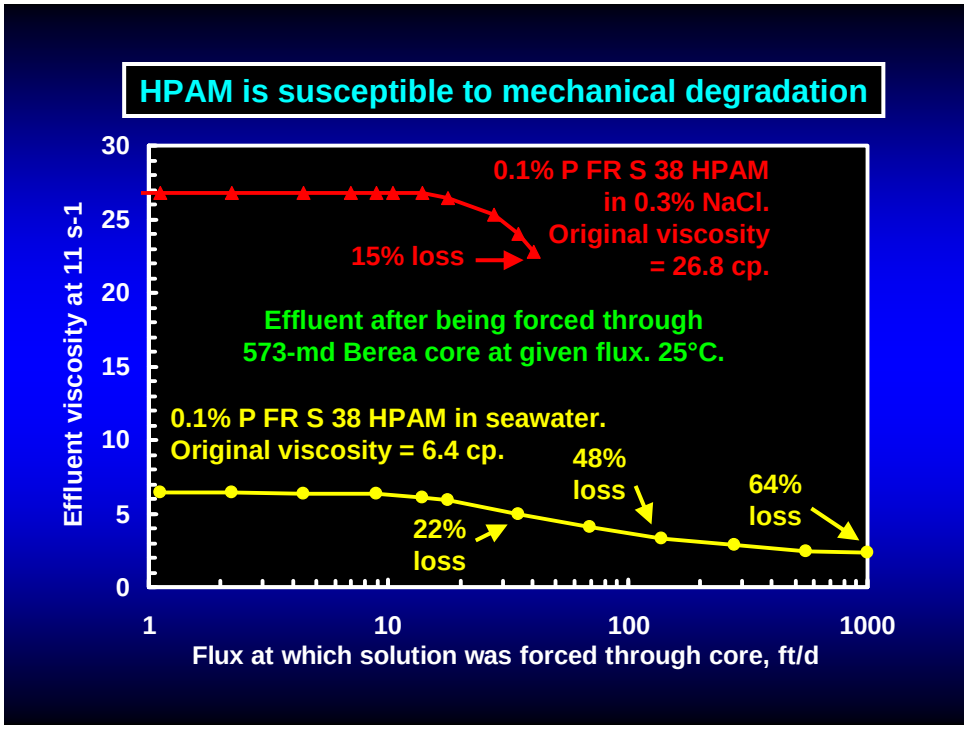

Fig. 11—Effluent viscosity versus flux for HPAM.

When an HPAM solution is injected into a well with no fractures (i.e., with radial flow as fluid moves away from the wellbore), the highest flux and the greatest mechanical degradation will occur just as the polymer enters the formation. Thereafter, fluxes will decrease and no further significant mechanical degradation of the polymer will occur (Seright *et al*. 1981, Seright 1983).

Consequently, Eqs. 3 and 4 are the type of relations that should be used when modeling rheology of HPAM solutions in porous rock. In the past, we often noted cases where commercial and academic simulators incorrectly assumed pseudoplastic behavior for HPAM solutions in porous media. Although HPAM solutions are well known to exhibit pseudoplastic behavior in viscometers, the petroleum literature (Pye 1964, Smith 1970, Jennings *et al*. 1971, Hirasaki and Pope 1974, Seright 1983) consistently revealed Newtonian or pseudodilatant behavior (resistance factor increases with increased flux) in porous rock (as shown in Fig. 10 for HPAM in 0.3% NaCl and in Fig. 12 for HPAM in seawater). The viscoelastic nature of the HPAM solutions in porous media overwhelms the pseudoplastic behavior seen in a viscometer. This point can be appreciated by examining the circle symbols in Fig. 10.

In Fig. 10, the circles plot viscosity versus shear rate (as measured in a viscometer) for fresh polymer solution (blue circles) and for polymer solution that was pre-sheared through the core using 41 ft/d flux (white circles). For this viscosity data, we plot the shear rate divided by 20 on the *x*-axis. We divided the shear rate by 20 because this empirical procedure allowed the viscosity versus shear rate data for xanthan (Fig. 8) to match the resistance factor versus flux data in ~550-md Berea. Other methods have been used to convert velocities in porous media to shear rates (Hirasaki and Pope 1974, Hejri *et al*. 1988, Cannella *et al*. 1988, Wreath *et al*. 1990, Seright 1991). Although disagreement exists on the most appropriate method, note that even if our shear-rate multiplier (i.e., 1/20) is varied by an order of magnitude either way, Newtonian or pseudodilatant behavior is seen in porous media when pseudoplastic behavior is seen in a viscometer.

In the power-law region, the slopes of the plots of *ln*(viscosity) versus *ln*(shear rate) were -0.36 (i.e., the power-law indexes were 0.64). However, the slopes of the plots of *ln*(resistance factor) versus *ln*(flux) in this same region were always zero or positive. In comparing viscosity data versus resistance factor data in Fig. 10, the most important point is that Newtonian or pseudodilatant behavior occurs in porous media for flux/shear rate values where pseudoplastic behavior is seen in a viscometer. At low flux values or shear rates, Newtonian behavior is seen in both porous rock and a viscometer.

For HPAM solutions in porous media, Newtonian and pseudodilatant rheology has often been reported in the literature (Pye 1964, Smith 1970, Jennings *et al*. 1971, Hirasaki and Pope 1974, Seright 1983, Masuda *et al*. 1992). One might try to argue the existence of a mild shear thinning behavior at low velocities for HPAM solutions in porous rock (Delshad *et al*. 2008). Although we suspect that pseudoplastic behavior for HPAM solutions can occur in very permeable sand and bead packs, our experience is that apparent pseudoplastic behavior is often an experimental artifact for HPAM solutions (with compositions that are practically used in chemical flooding applications) in porous rock (with less than one darcy permeability). Pseudoplastic behavior may seem to occur at low rates for HPAM solutions in porous rock (1) if sufficiently accurate pressure transducers are not used (we use Honeywell ST-3000™ quartz transducers), (2) if temperature is not controlled, and (3) if the polymer molecular weight is too high to propagate without forming an internal or external filter cake (i.e., if the polymer contains significant concentrations of "microgels" or high molecular weight species that are too large to flow efficiently through the pore structure). For the latter case, the micorgels or high molecular weight species cannot be expected to propagate very far into the porous rock of a reservoir. They are either mechanically degraded into smaller species (Seright *et al*. 1981) or they are retained by the rock fairly close to the injection rock face (Chauveteau and Kohler 1984).

Fig. 12 plots coreflood results that are analogous to Fig. 10, except using 0.1% P FR S 38 HPAM in seawater (4.195% TDS) instead of 0.3% NaCl. Qualitatively, the behavior was quite similar to that seen in Fig. 10. When injecting fresh polymer solution at low flux (0.14 to 1.1 ft/d, red circles in Fig. 12), resistance factors averaged 7.9 and showed Newtonian behavior. This resistance factor value was 23% greater than the viscosity (6.4 cp) for this solution (which showed nearly Newtonian behavior in a viscometer). As flux was increased from 1.1 to 14 ft/d, resistance factors increased to 42 (again, red circles in Fig. 12). Resistance factor versus flux from 0.14 to 14 ft/d was described reasonably well using Eq. 5 (blue solid curve in Fig. 12).

$$F_r = 7.9 + u^2/5.6 \quad (5)$$

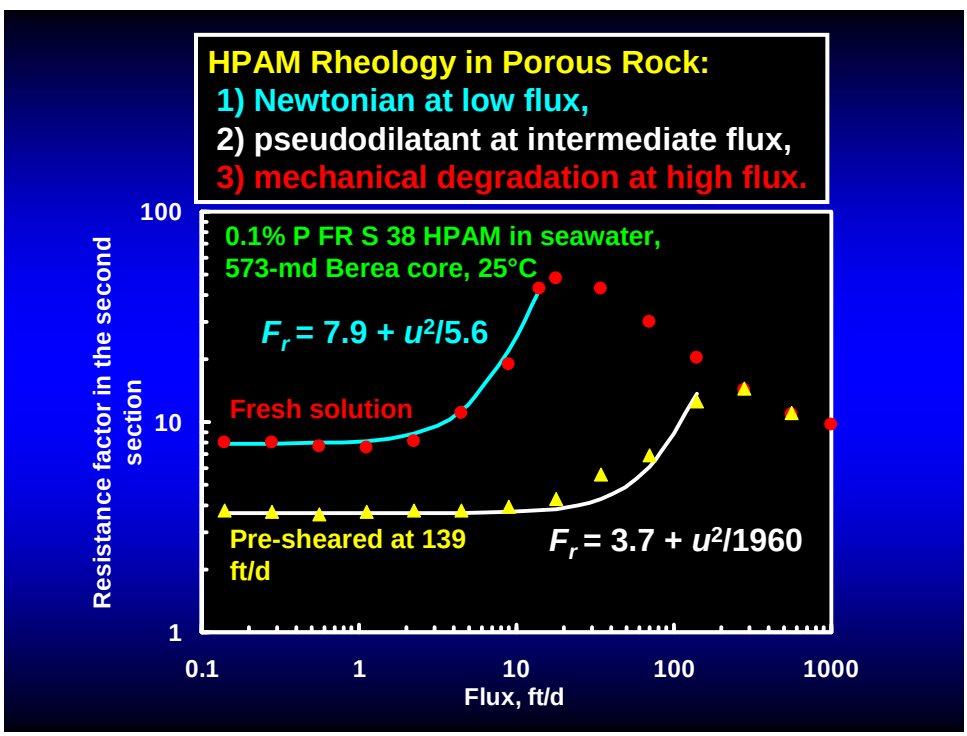

Fig. 12—Resistance factor versus flux for HPAM in seawater.

For flux values up to 14 ft/d (pressure gradients up to 30 psi/ft), effluent from the core exhibited no loss of viscosity, as compared with fresh polymer solution and as measured at a shear rate of 11 s^{-1}, 25°C (yellow circles in Fig. 11). For higher fluid velocities, effluent viscosities decreased, with a 22%

viscosity loss seen at a flux of 35 ft/d (pressure gradient of 475 psi/ft) and a 64% viscosity loss at a flux of 1,000 ft/d (pressure gradient of 3,280 psi/ft). Resistance factors appear to go through a maximum at 18 ft/d (red circles in Fig. 12). Again, the decline in resistance factor for flux values above the maximum occurs because of polymer mechanical degradation (Seright 1983). If polymer effluent from 139 ft/d (938 psi/ft) is re-injected at a series of lower rates (yellow triangles in Fig. 12), resistance factors show a monotonic decrease with decreasing flux—approaching 3.7 at the lowest fluxes. This resistance factor value was 12% greater than the viscosity (3.3 cp) for this solution. Resistance factor versus flux for this re-injected solution was described reasonably well using Eq. 6 (white curve in Fig. 12).

$$F_r = 3.7 + u^2/1960 \quad (6)$$

Entrance Pressure Drop. Previous work (Seright 1983) revealed that HPAM solutions can exhibit an entrance pressure drop, associated with the polymer entering the porous medium. Entrance pressure drop is zero until the polymer solution flux increases to the rate where mechanical degradation takes place. Thereafter, entrance pressure drop and the degree of polymer mechanical degradation increase with increasing flux. In addition, polymer solutions that undergo a large entrance pressure drop and a high degree of mechanical degradation when first injected into a core show little or no entrance pressure drop and little additional degradation after re-injection into the same core at the same or lower flux. These findings were confirmed during our current studies with 0.1% P FR S 38 HPAM solutions (Fig. 13). Interestingly for fresh HPAM in both seawater and 0.3% NaCl brine, the onset for mechanical degradation and the entrance pressure drop occurs at a flux about 14 ft/d (yellow and red curves in Fig. 13). The existence of an entrance pressure drop decreases injectivity for HPAM solutions (Seright 1983).

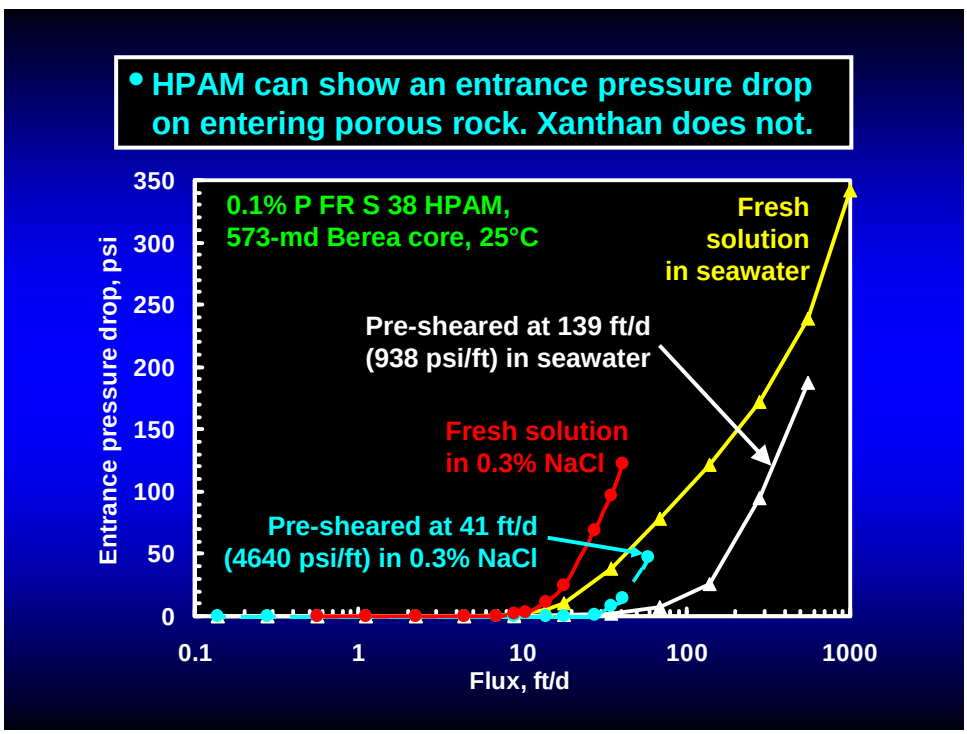

Fig. 13—Entrance pressure drop versus flux for HPAM in seawater.

Incidentally, the two resistance factor data curves in Fig. 10 and the two resistance factor data curves in Fig. 12 were all obtained using the same 573-md Berea core. No attempts were made to "clean" the core between injection stages. No significant face plugging was noted during the course of these floods—due to the cleanliness of the polymer used and the moderate total throughput values used. Our experience both in this work and in previous work (Seright 1983) is that mechanical degradation of HPAM polymers is dominated by the pressure gradient applied through the porous medium and is fairly insensitive to the time or distance that the polymer is exposed to a given pressure gradient (Seright

1983). All expermiments described here were performed at room temperature (~25°C). However, we have observed the same phenomenon and behavior during additional experiments performed at 41°C, 60°C, and 85°C. Consistent with other work (Liauh and Liu 1984), barring chemical or thermal degradation, resistance factors (apparent viscosity in porous media relative to water) are fairly insensitive to temperature.

Injectivity Losses and Fracture Extension

In this section, we consider the implications of previous experimental observations on injectivity of polymer solutions in field applications. Pang and Sharma (1997) categorized plugging behavior in four classes, depending on the shape of a plot of "inverse injectivity decline" versus volume throughput. These plots were indicative of whether the filter cake was external (i.e., formed on the rock face) or internal (i.e., formed by physical trapping of particles within the rock), compressible or incompressible, or some combination. Our data appears to be dominated by formation of compressible external filter cakes—because the filter cake resistance increases sharply with increased throughput (e.g., Figs. 1 and 4-7) and the resistance increase within the rock is small compared to that on the rock surface (Fig. 1).

Saripalli *et al*. (1999) and Gadde and Sharma (2001) considered fracture growth as a function of particle plugging and other effects. Their work demonstrated that particle plugging during injection at a fixed rate leads to fracture extension. As a portion of the fracture face becomes impaired by plugging, pressure at the fracture tip forces the fracture to extend until enough fracture area is available to accommodate the existing injection rate. Consequently, injectivity observed for a well [i.e., injection rate divided by (flowing pressure minus static pressure)] may not appear to be sensitive to volume of particles injected (Schmidt *et al*. 1999). Similarly, when injecting viscous polymer solutions, fracture extension explains why injectivity often appears to be not greatly different than that during water injection (Wang *et al*. 2008).

Injection above the formation parting pressure and fracture extension is not necessarily detrimental. Under the proper circumstances it can increase fluid injectivity, oil productivity, and reservoir sweep efficiency (Crawford and Collins 1954, Dyes *et al*. 1958, Wang *et al*. 2008). The key is to understand the degree of fracture extension for a given set of injection conditions so that fractures do not extend out of the target zone or cause severe channeling. Thus, we are interested in whether fractures must be present to accommodate injection of EOR polymer solutions and the degree to which fractures can be expected to extend.

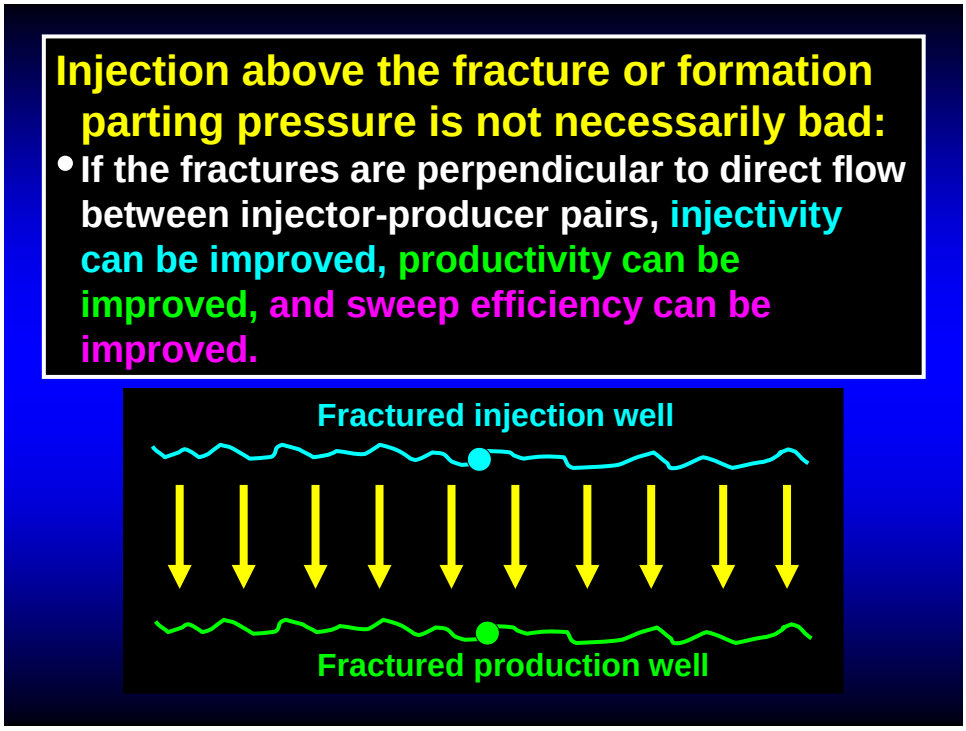

Injection above the fracture or formation parting pressure is not necessarily bad:

- Even if the fractures point directly between injector-producer pairs, injectivity can be improved, productivity can be improved, and sweep efficiency can be improved.

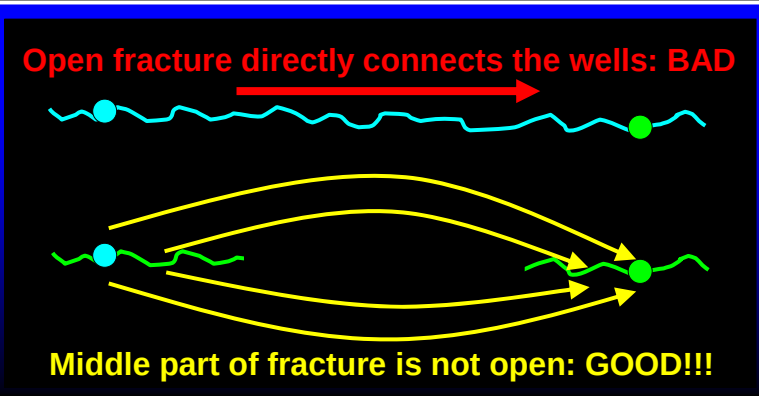

dp/dl for an Open Fracture Between Wells.

A 1-mm open fracture between two wells allows high injection/production rates but also allows severe channeling. SPE 99441.

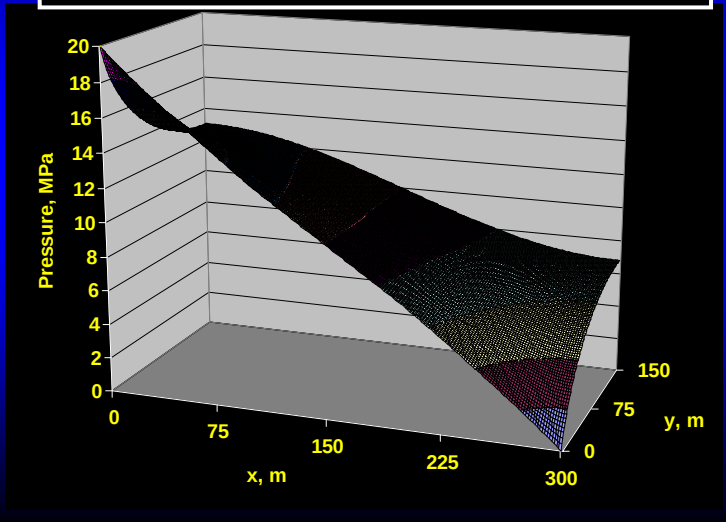

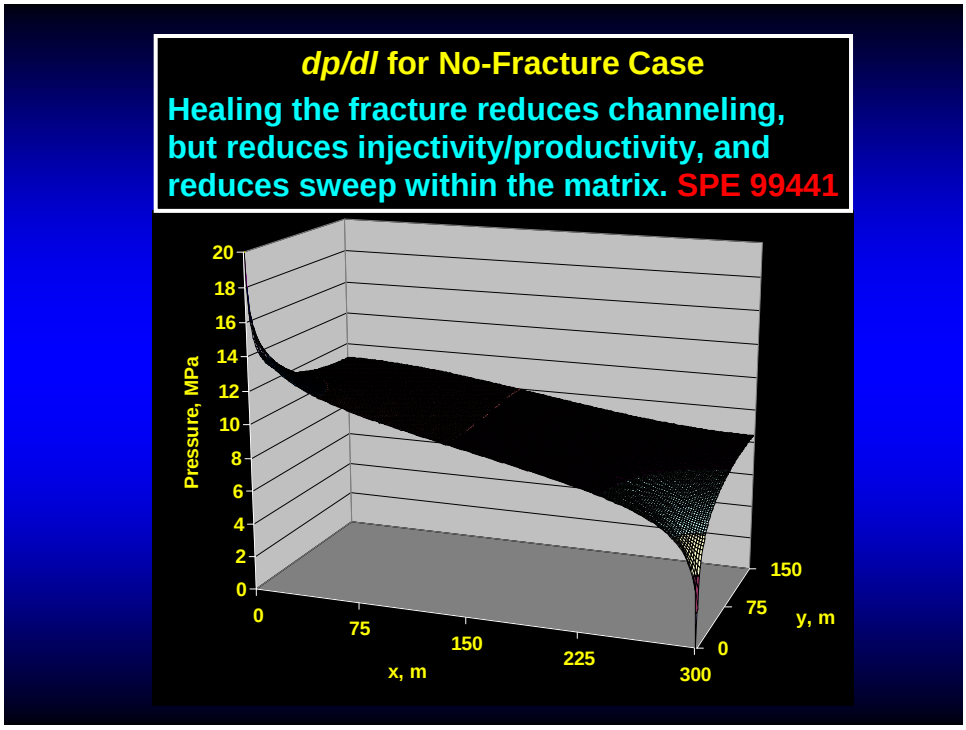

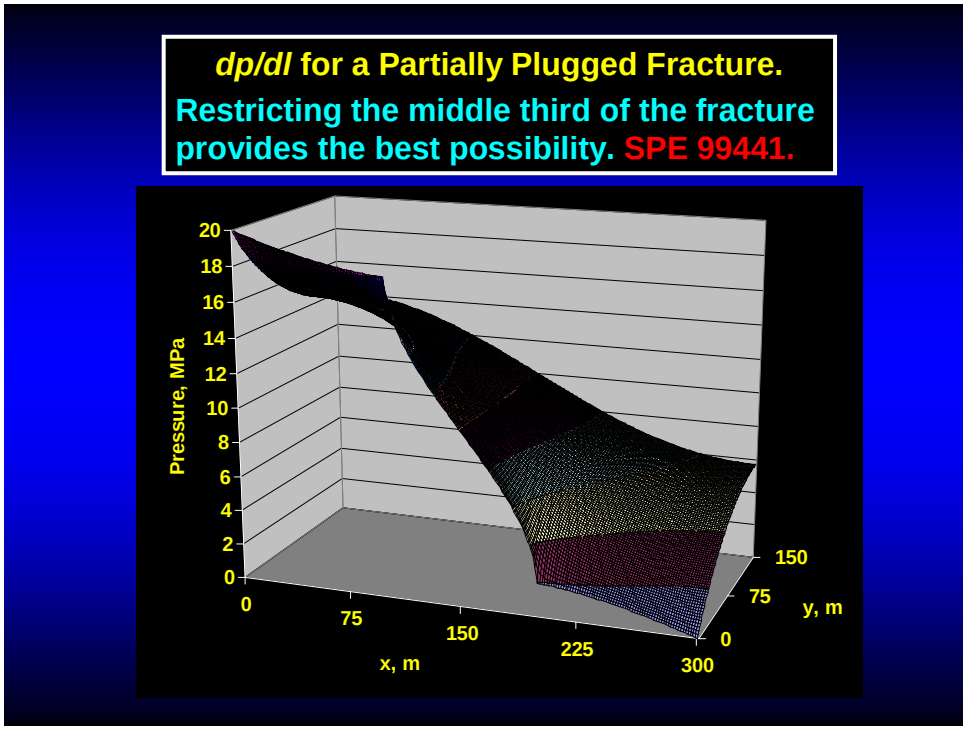

Filterability (Face Plugging). For various well configurations, we calculated throughput values as a function of pore volumes of polymer solution injected. (To emphasize face plugging effects, solution viscosities were assumed to be only 1-cp.) Results are shown in Fig. 14. For the base case, we used a 20-acre 5-spot pattern with a well bore radius (r_w) of 0.375 ft and porosity of 0.2. (These calculations are independent of formation permeability, injection rate, and injection pressure. They are also not dependent on formation height for vertical wells, although they are sensitive to height for unfractured horizontal wells. They are dependent on wellbore radius, type of completion, the presence of fractures, and fracture length.)

Unfractured Vertical Wells. The red dashed curve in Fig. 14 show throughput values for a vertical well with an open hole completion (no fracture). For this case, throughput values exceeded 10,000 cm^3/cm^2 before 0.01 *PV* of polymer solution was injected. Combined with Figs. 6 and 7, the results suggest that rock face plugging will become severe quite quickly during polymer injection into vertical wells that do not intersect fractures or void features. These results assumed an open-hole completion. Plugging is expected to be more severe for wells completed with perforations, since the sand face area is more restricted. Since many polymer floods have been reported without significant plugging (Manning *et al.* 1983, Seright 1993), the implication is that most injection wells during polymer flooding may intersect fractures or formation parts. This suggestion is consistent with a statement by Van den Hoek *et al.* 2008: "It is well established within the industry that water injection mostly takes place under induced fracturing conditions. Particularly, in low-mobility reservoirs, large fractures may be induced during the field life." Because polymer solutions are more viscous than water, injection above the formation parting pressure will be even more likely during a polymer flood than during a waterflood.

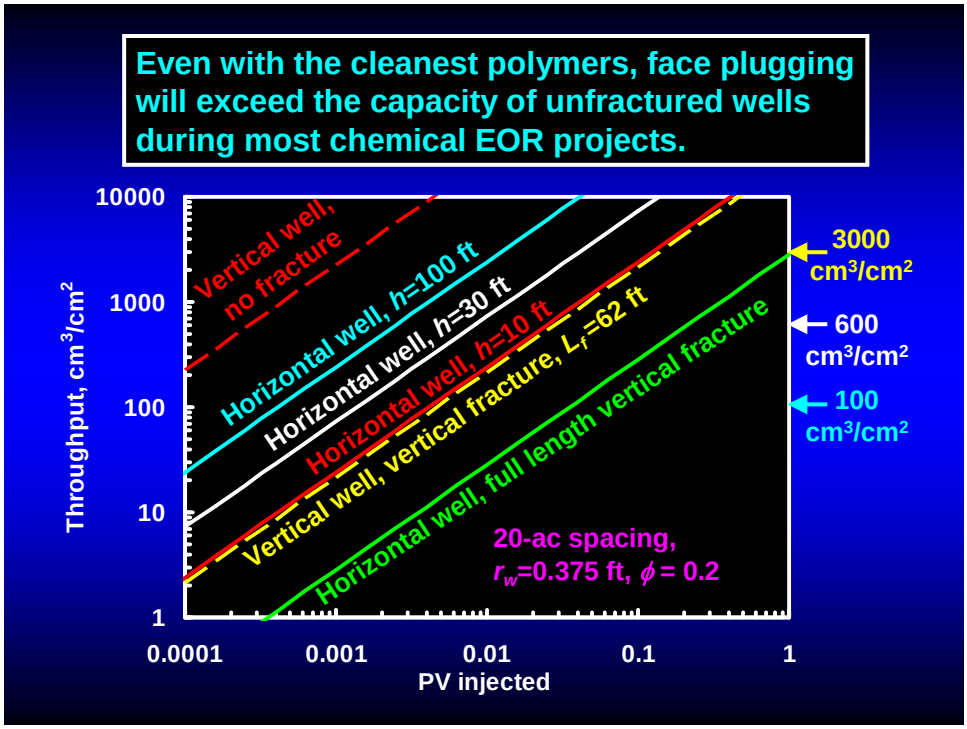

Fig. 14—Throughput versus *PV* injected for various cases.

Unfractured Horizontal Wells. The solid blue, white, and red lines in Fig. 14 plot results for unfractured, open hole horizontal wells where the well length spans the entire pattern (933 ft for the case of 20-acre spacing). Three formation height values (*h*) were considered, from 10 to 100 ft. Again, considering the polymers shown in Figs. 6 and 7, satisfactory injection of more than 0.1 *PV* could only be expected for the cleanest polymers (i.e., that do not plug before 1,000 cm^3/cm^2 throughput), without inducing fractures (or formation parts for unconsolidated sands).

Vertical Fractures in Vertical and Horizontal Wells. The yellow dashed line in Fig. 14 shows the case for a vertical well with a two-wing fracture, where each fracture wing is 62 ft long (L_f=62 ft). This case allows injection of more than 0.1 *PV* of polymer solution without exceeding the maximum throughput limits associated with the cleanest polymers from Figs. 6 and 7. If plugging of the fracture faces occurred, the fractures are expected to grow in length (and possibly in height) to accommodate additional fluid injection (Pang and Sharma 1997). The green line in Fig. 14 shows the extreme case where a vertical fracture has grown to span the entire pattern (i.e., growing to pass midway between production wells, so that severe channeling does not result). This case for a pattern-spanning fracture

that intersects a vertical injection well is identical to that for a vertical fracture that follows the entire length of a pattern-spanning horizontal injector. As revealed in Fig. 14, this case allows injection of an entire pore volume of polymer solution for those polymers that show the least plugging in Figs. 6 and 7 (i.e., X US K K36 xanthan, 0.1% P FR S 38 HPAM, and 0.1% P CH H H22 HPAM). Naturally fractured reservoirs could have tremendous sand face surface area—much more than the most optimistic case shown in Fig. 14.

Fracture Growth Resulting from Face Plugging. Fracture growth resulting from injection of particulates during waterflooding has been studied by others (Sharma et al. 2000, Saripalli *et al*. 1999, Gadde and Sharma 2001), including the effects of thermal stresses and pore pressure. Here, we focus on fracture growth due to injection of polymer solutions with a simplified analysis. In particular, we assumed (1) severe face plugging occurs (i.e., filter cake resistance rises to high values) suddenly at throughput values of 100, 600, or 3,000 cm^3/cm^2 (reflecting the behavior observed in Figs. 6 and 7), (2) the vertical well has a two-wing fracture, (3) injection rate is fixed, (4) as plugging of the fracture faces occurs, the fracture extends to maintain a fixed pressure at the fracture tip, (5) pressure losses from the well to the fracture tip are negligible, and (6) the injectant has the same viscosity as water. Fig. 15 shows the results of this analysis. During polymer floods that use bank sizes from 0.1 to 0.6 *PV*, fracture extension is expected to be severe using polymers that plug with 100 cm^3/cm^2 throughput, substantial using polymers that plug with 600 cm^3/cm^2 throughput, and moderate using polymers that plug with 3,000 cm^3/cm^2 throughput.

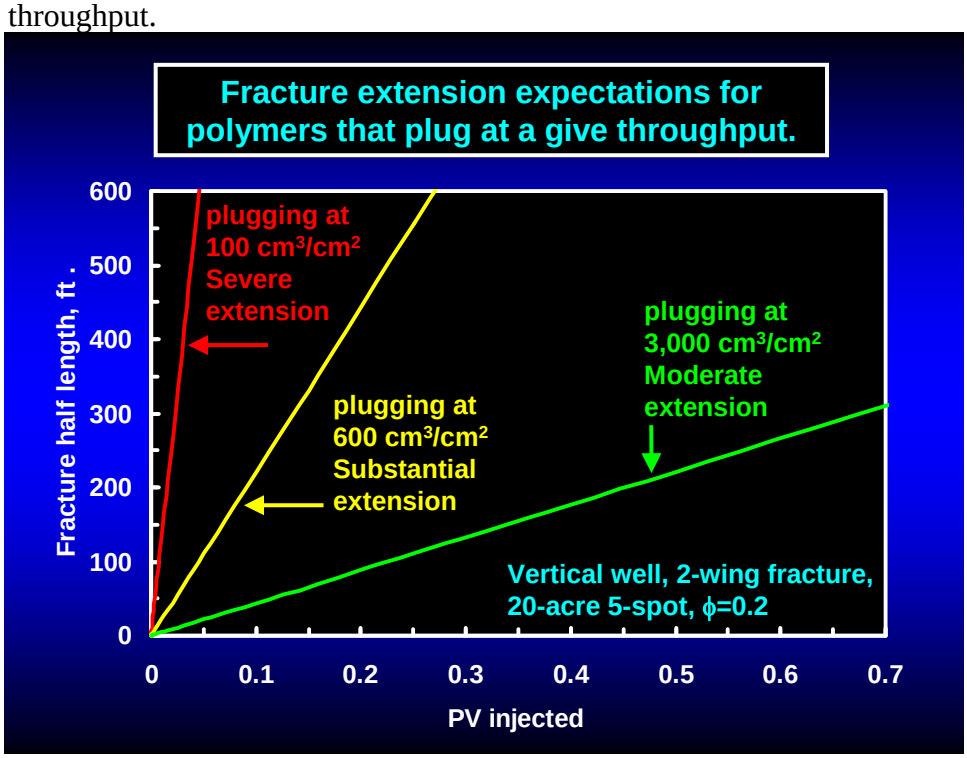

Fig. 15—Fracture extension versus filter cake resistance in a vertical well.

Anticipated Injectivity Losses for Viscous Fluids in Unfractured Wells. If a viscous fluid is injected into a well with no fractures or formation parts, simple physics dictates that the injectivity (injection rate divided by downhole pressure difference between the well and the formation) must decrease. In Fig. 16, the dashed curves show the predicted injectivities (relative to 1-cp water) for Newtonian fluids with viscosities ranging from 3 to 100 cp. After injecting 0.1 *PV* of viscous Newtonian solution, the anticipated injectivity losses were 64% for 3-cp fluid, 89% for 10-cp fluid, 96% for 30-cp fluid, and almost 99% for 100-cp fluid. For comparison, the solid curves with symbols show the predicted injectivities for 0.1% solutions of xanthan or HPAM, based on Eqs. 2, 4, and 6 (and assuming 1,000 psi pressure drop from the wellbore to the external drainage radius). For these cases, injectivity losses at 0.1 *PV* ranged from 83% to over 98%. The central point from Fig. 16 is that substantial injectivity losses

must be expected during polymer injection into any well that does not intersect fractures or fracture-like features (unless the injectant reduces the residual oil saturation and substantially increases the relative permeability to water). Since injectivity reductions of this magnitude are often economically unacceptable, fractures or fracture-like features are expected to open and extend significantly during the course of most polymer floods. Thus, an understanding of the orientation and growth of fractures appears crucial for most EOR projects where polymer solutions are injected.

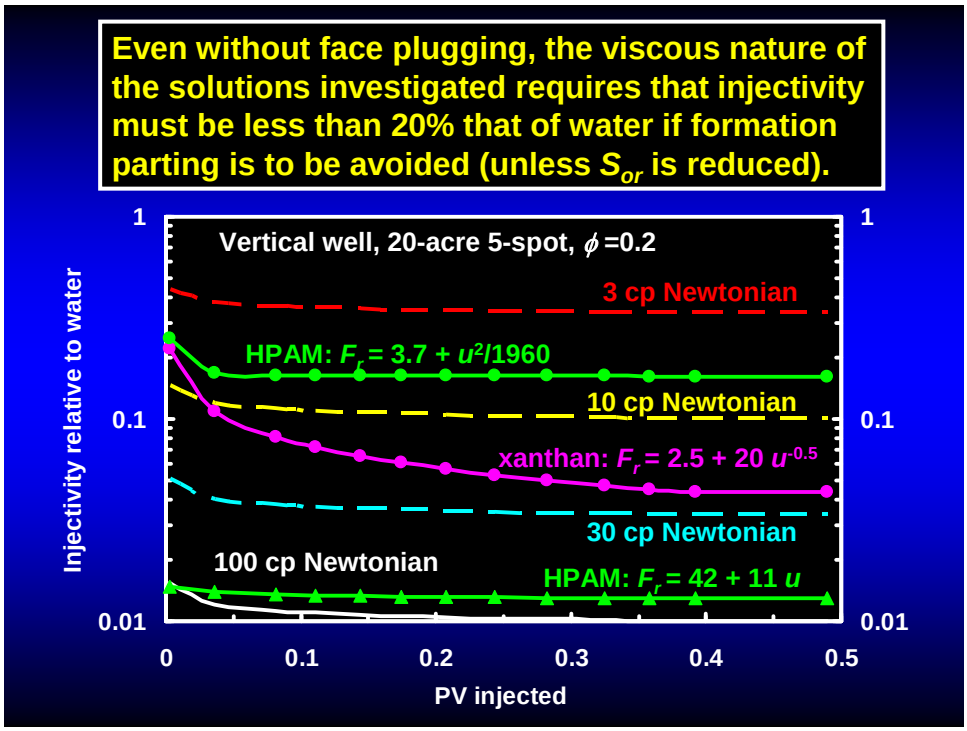

Fig. 16—Injectivity losses expected for viscous injectants in an unfractured vertical well.

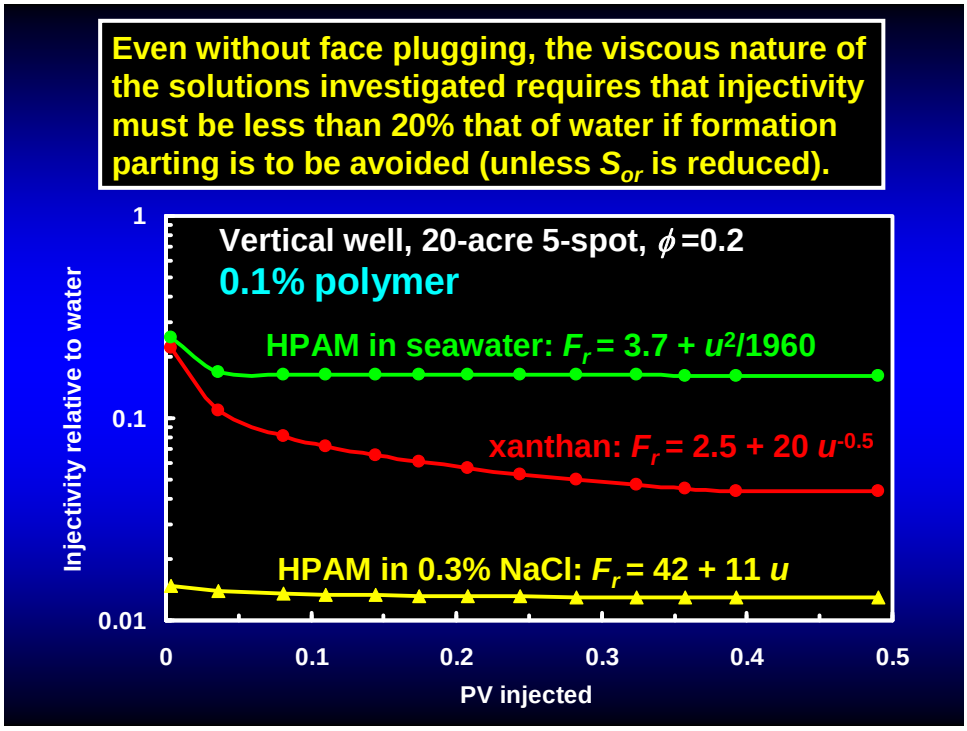

Fracture Growth Resulting from Injecting a Viscous Fluid. The previous two sections predicted

substantial injectivity losses during typical polymer floods in wells that do not intersect fractures. Consequently, utilizing fractures to enhance injectivity may be a practical necessity during many (perhaps most) field applications of chemical flooding, where polymers are used for mobility control. In the Daqing field (permeability ~1 darcy) in China, site of the world's largest polymer flood, Wang *et al*. 2008 demonstrated that strategic use of fractures in wells during a polymer flood can substantially enhance (1) polymer solution injectivity, (2) oil productivity, and (3) sweep efficiency. Of course, if fractures or formation parts are used for this purpose, care must be exercised so that the fractures do not extend out of zone or cause severe channeling.

We performed a simple analysis to estimate the degree of fracture extension that might result from injecting viscous fluids. In this analysis, we assumed (1) the vertical well has a two-wing fracture, (2) injection rate is fixed, (3) no plugging of the fracture faces occurs, (4) as the viscous fluid leaks off farther in the porous rock, the fracture extends laterally (not vertically) to maintain a fixed pressure at the fracture tip, (5) pressure losses from the well to the fracture tip are negligible, and (6) the polymer rheological relations in Eqs. 2-6 are applicable. Fig. 17 shows the results of this analysis. In this simple analysis, the fracture half length jumps from 0 to 62 ft when the fracture first opens. This result occurs because of switching from the radial Darcy equation to the linear Darcy equation. For the four HPAM cases (Eqs. 3-6), the area associated with the minimum fracture half lengths (62 ft) usually reduced the flux values to the point where polymer solution rheology was Newtonian in the porous rock (i.e., with resistance factors of 3.7, 7.9, 42, or 65 for the various HPAM cases in Fig. 17). For the xanthan case, resistance factors in the porous rock continually increased as the fractures extended. (Recall that our injection rate was fixed.) Because our calculations assumed that resistance to flow down the fractures was negligible (i.e., infinite fracture conductivity), the results in Fig. 17 may overestimate fracture growth if the fractures are relatively narrow or filled with a proppant that significantly reduces fracture conductivity. The calculations assumed 1,000 psi pressure difference between the fracture and pore pressure deep within the formation. Strictly speaking, the calculations apply to 25°C, since the resistance factor data were measured at room temperature. However, barring chemical or thermal degradation of the polymer, the resistance factor behavior should be fairly insensitive to temperature (Liauh and Liu, 1984).

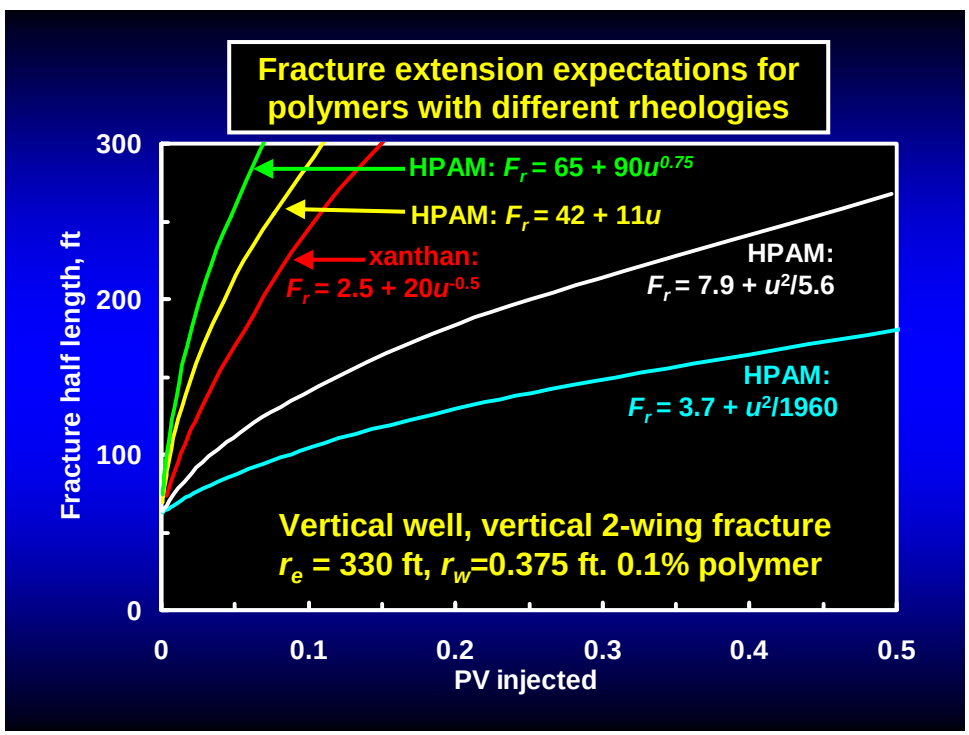

Fig. 17—Extension of fracture lengths when injecting polymer solutions.

A key point from Figs. 15 and 17 is that fractures or fracture-like features are expected to open and extend significantly during the course of most polymer floods. Thus, an understanding of the orientation and growth of fractures appears crucial for most EOR projects where polymer solutions are injected.

The need for injection above the formation parting pressure will be mitigated if a formulation (e.g., microemulsion, surfactant formulation, or ASP formulation) is injected that reduces the residual oil saturation to near zero near the wellbore. By mobilizing all or nearly all oil, the relative permeability to the aqueous phase can be increased by a factor from 2 to 20, depending on circumstances. This effect may eliminate the need to inject above the formation parting pressure, or alternatively, mitigate the degree of fracture extension if fractures are open during injection of the EOR fluid.

Conclusions

This paper examined the three principal EOR polymer properties that affect injectivity: (1) debris in the polymer, (2) polymer rheology in porous media, and (3) polymer mechanical degradation. We also examined the impact of fractures on polymer solution injectivity.

1. We developed an improved test to measure the tendency of EOR polymers to plug porous media. The new test demonstrated that plugging tendencies varied considerably among both partially hydrolyzed polyacrylamide (HPAM) and xanthan polymers.
2. Rheology and mechanical degradation in porous media were quantified for a xanthan and an HPAM polymer. Consistent with previous work, we confirmed that xanthan solutions show pseudoplastic behavior in porous rock that closely parallels that in a viscometer. Xanthan was remarkably resistant to mechanical degradation, with a 0.1% xanthan solution (in seawater) experiencing only a 19% viscosity loss after flow through 102-md Berea at 24,600 psi/ft pressure gradient.
3. For 0.1% HPAM in both 0.3% NaCl brine and seawater in 573-md Berea, Newtonian behavior was observed at low to moderate fluid fluxes, while pseudodilatant behavior was seen at moderate to high fluxes. No evidence of pseudoplastic behavior was seen in the porous rock, even though one solution exhibited a power-law index of 0.64 in a viscometer. For this HPAM in both brines, the onset of mechanical degradation occurred at a flux of 14 ft/d in 573-md Berea sandstone.
4. Considering the polymer solutions investigated, satisfactory injection of more than 0.1 *PV* in field applications could only be expected for the cleanest polymers (i.e., that do not plug before 1,000 cm^3/cm^2 throughput), without inducing fractures (or formation parts for unconsolidated sands).
5. Even in the absence of face plugging, the viscous nature of the solutions investigated requires that injectivity must be less than one-fifth that of water if formation parting is to be avoided. Since injectivity reductions of this magnitude are often economically unacceptable, fractures or fracture-like features are expected to open and extend significantly during the course of most polymer floods. Thus, an understanding of the orientation and growth of fractures may be crucial for EOR projects where polymer solutions are injected. Of course, surfactant floods that mobilize most near-wellbore oil and increase relative permeabilities to near unity may reduce the need for injection above the formation parting pressure or alternatively, mitigate the degree of fracture extension if fractures are open during injection of the EOR fluid.

CONCLUSIONS

1. We developed an improved test of the tendency for EOR polymers to plug porous media. The new test is more sensitive to differences in polymer plugging than the old 1970s test. The new test demonstrated that plugging tendencies varied considerably among both partially hydrolyzed polyacrylamide (HPAM) and xanthan polymers.

2. Consistent with previous work, we confirmed that xanthan solutions show pseudoplastic behavior in porous rock that closely parallels that in a viscometer. Xanthan was remarkably resistant to mechanical degradation, with a 0.1% xanthan solution (in seawater) experiencing only a 19% viscosity loss after flow through 102-md Berea sandstone at a pressure gradient of 24,600 psi/ft.

CONCLUSIONS

3. For 0.1% HPAM in both 0.3% NaCl brine and seawater in 573-md Berea sandstone, Newtonian behavior was observed at low to moderate fluid fluxes, while pseudodilatant behavior was seen at moderate to high fluxes. No evidence of pseudoplastic behavior was seen in the porous rock, even though one solution exhibited a power-law index of 0.64 in a viscometer. For this HPAM in both brines, the onset of mechanical degradation occurred at a flux of 14 ft/d in 573-md Berea sandstone.

CONCLUSIONS

4. Considering the polymer solutions investigated, satisfactory injection of more than 0.1 PV in field applications could only be expected for the cleanest polymers (i.e., that do not plug before 1,000 cm^3/cm^2 throughput), without inducing fractures (or formation parts for unconsolidated sands).

5. Even in the absence of face plugging, the viscous nature of the solutions investigated requires that injectivity must be less than one-fifth that of water if formation parting is to be avoided. Since injectivity reductions of this magnitude are often economically unacceptable, fractures or fracture-like features are expected to open and extend significantly during the course of most polymer floods. Thus, an understanding of the orientation and growth of fractures appears crucial for most EOR projects where polymer solutions are injected.

Do HPAM Solutions Show Shear Thinning Behavior In Porous Rock?

- The theoretical possibility was raised by Hirasaki and Pope in 1974 and often pushed as fact since then.
- Most commercial and academic polymer and chemical flooding simulators assume shear thinning behavior.
- Most literature reports show no evidence of shear thinning for HPAM solutions in porous rock.
- A few authors have reported minor levels of shear thinning at very low velocities in porous rock.

Is shear thinning for HPAM in porous rock real or just an experimental artifact?

Hirasaki and Pope: *JPT* (Aug. 1974) 340

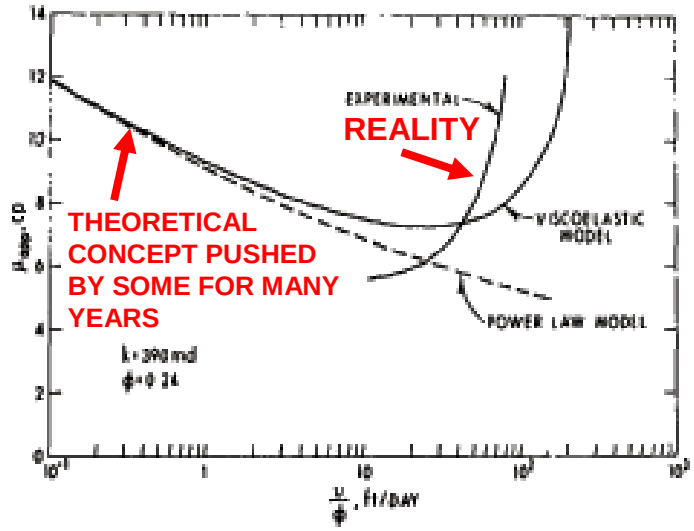

FIG. 5 — RHEOLOGICAL BEHAVIOR OF 0.15 PERCENT POLYOX WSR-301 IN GALLUP CORE.

Jennings, Rogers and West: *JPT* (March 1971) 395

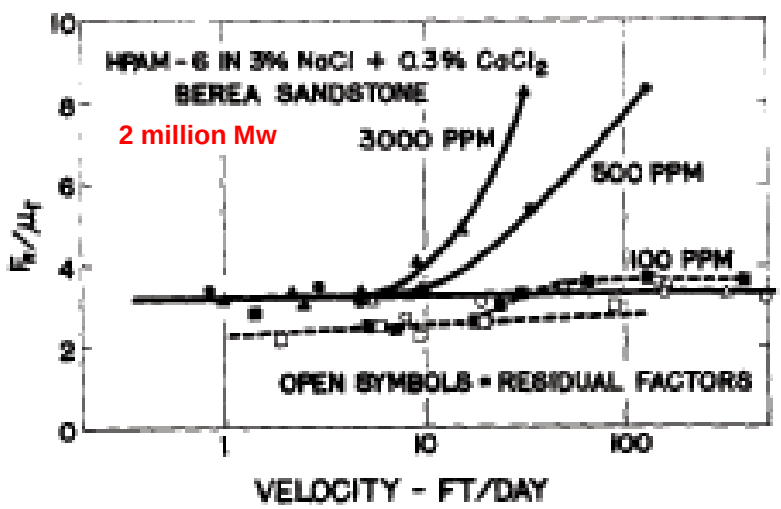

Fig. 8—Effect of HPAM concentration on the resistance factor.

Jennings, Rogers and West: *JPT* (March 1971) 394

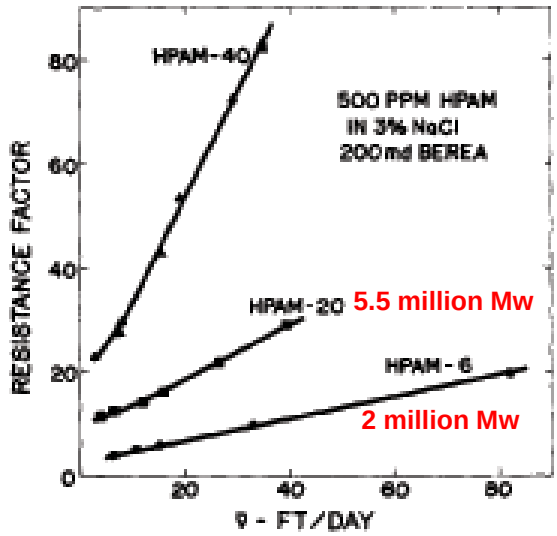

Fig. 6—Viscoelastic behavior in Berea sandstone of solutions of different molecular weights of HPAM.

Jennings, Rogers and West: *JPT* (March 1971) 395

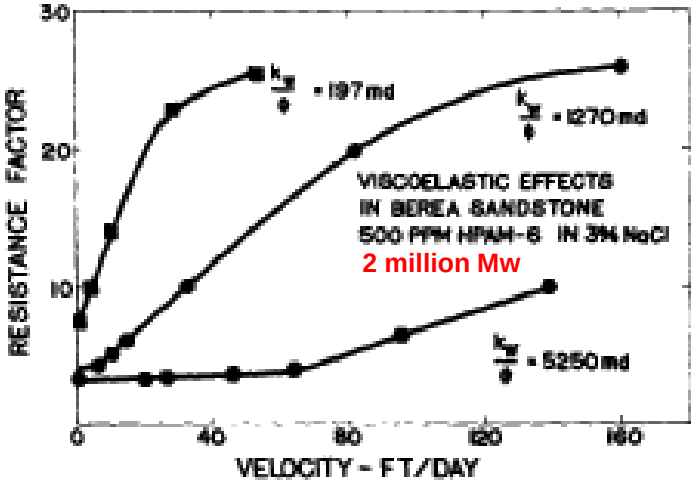

Fig. 7—Flow of a hydrolyzed polyacrylamide solution through sandstones of different effective pore sizes.

Jennings, Rogers and West: *JPT* (March 1971) 394

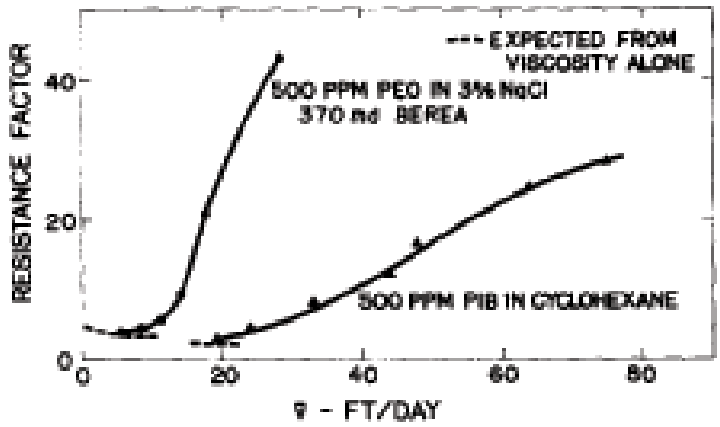

Fig. 5—Viscoelastic behavior of polyisobutylene and polyethylene oxide solutions in Berea sandstone.

D. J. Pye: *JPT* (Aug. 1964) 912

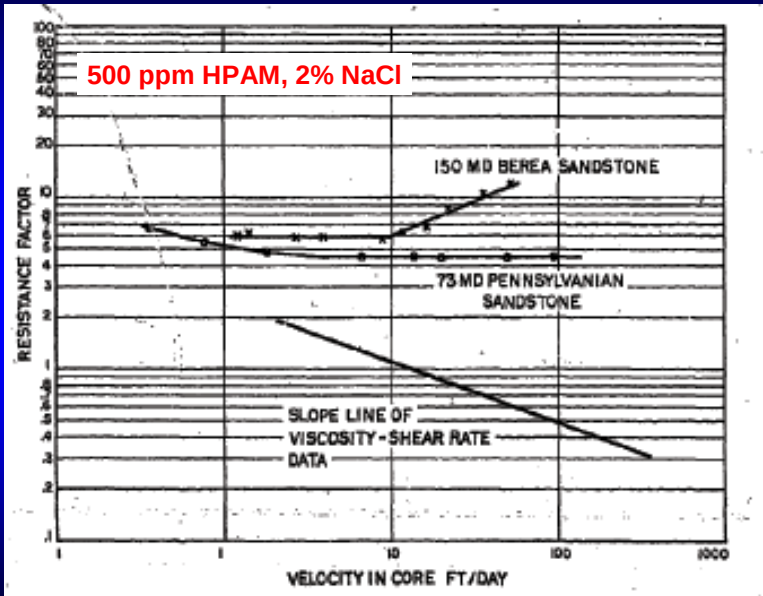

Fig. 2—Effect of Flooding Velocity on Resistance Factor.

Is shear thinning for HPAM in porous rock real or just an experimental artifact?

- Most literature reports show no evidence of shear thinning for HPAM solutions in porous rock.
- A 1981 UT MS student reported minor levels of shear thinning at low velocities with 0.1% Pusher 700 in Berea (50% increase in F_r with 10X decrease in rate).
- An apparent shear thinning can be seen in porous rock as an experimental artifact (a) if insensitive pressure transducers are used, (b) if temperature is not controlled, (c) if microgels penetrate into the core.
- Microgels will either be destroyed by mechanical degradation or removed by retention.

OBSERVATIONS FOR HPAM SOLUTIONS

- The concept that HPAM solutions show significant shear thinning in porous rock during polymer or chemical flooding in field applications is usually wrong.
- Shear thickening behavior is real and should be included when modeling rheology in rock if high velocities occur.
- In the absence of real supporting data, it would be better (less wrong) to assume only Newtonian (velocity independent) behavior than to assume only shear thinning behavior when modeling rheology in porous rock.

Nomenclature

A = area, ft^2 [m^2]
F_r = resistance factor (water mobility/polymer solution mobility)
h = formation height, ft [m]
k = permeability to brine or water, darcys [μm^2]
k_m = matrix permeability, darcys [μm^2]
k_s = filter cake permeability, darcys [μm^2]
L = length, ft [m]
L_f = fracture half length, ft [m]
l_s = filter cake thickness, ft [cm]

PV = pore volumes of fluid injected
Δp = pressure drop, psi [Pa]
q = injection rate, bbl/day, [m^3/day]
r_e = external drainage radius, ft [m]
r_w = wellbore radius, ft [m]
μ = viscosity, cp [mPa-s]
μ_w = water viscosity, cp [mPa-s]
ϕ = porosity

References

Burnett, D.B. 1975: "Laboratory Studies ot Biopolymer Injectivity Behavior Effectiveness of Enzyme Clarification," Paper SPE 5372 presented at the California Regional Meeting, Ventura, California, 2-4 April.

Cannella, W.J., Huh, C., and Seright, R.S. 1988. Prediction of Xanthan Rheology in Porous Media. Paper SPE 18089 presented at the SPE Annual Technical Conference and Exhibition, Houston, Texas, 2–5 October.

Chauveteau, G. 1982. Rodlike Polymer Solution Flow through Fine Pores: Influence of Pore Size on Rheological Behavior. *J. Rheology* **26**(2): 111–142.

Chauveteau, G. and Kohler, N. 1984. Influence of Microgels in Polysaccharide Solutions on Their Flow Behavior Through Proous Media, *SPEJ* **24**(3): 361-368.

Crawford, P.B. and Collins, R.E. 1954. Estimated Effect of Vertical Fractures on Secondary Recovery. *Trans.*, AIME, **201**: 192–196.

Delshad, M., Kim, D.H., Magbagbeolz, O.A., Huh, C., Pope, G.A., and Tarahhom, F. 2008. Mechanistic Interprretation and Utilization of Viscoselastic Behavior of Polymer Solutions for Improved Polymer-Flood Efficiency. Paper SPE 113620 presented at the SPE/DOE Improved Oil Recovery Symposium, Tulsa, Oklahoma, 19–23 April.

Duane, N.C. and Dauben, D.L. 1983. Evaluation of the Coalinga Polymer Demonstration Project. Contract No. DOE/BC/10033-7, US DOE, Washington, D.C.

Dyes, A.B., Kemp, C.E., and Caudle, B.H. 1958. Effect of Fractures on Sweep-out Pattern. *Trans.*, AIME **213**: 245–249.

Gadde, P.B. and Sharma, M.M. 2001. Growing Injection Well Fractures and Their Impact on Waterflood Performance. Paper SPE 71614 presented at the SPE Annual Technical Conference and Exhibition, New Orleans, Louisiana, 30 September–3 October.

Hejri, S., Willhite, G.P., and Green, D.W. 1988. Development of Correlations to Predict Flocon 4800 Biopolymer Mobility in Porous Media. Paper SPE 17396 presented at the SPE/DOE Enhanced Oil Recovery Symposium, Tulsa, Oklahoma, 17–20 April.

Hirasaki, G.J., and Pope, G.A. 1974. Analysis of Factors Influencing Mobility and Adsorption in the Flow of Polymer Solution Through Porous Media. *SPEJ* **14**(4): 337–346.

Jennings, R.R., Rogers, J.H., and West, T.J. 1971. Factors Influencing Mobility Control by Polymer Solutions. *JPT* **23**(3): 391–50, SPE 2867-PA.

Levitt, D. B. and Pope, G.A. 2008. Selection and Screening of Polymers for Enhanced-Oil Recovery. Paper SPE 113845 presented at the SPE/DOE Improved Oil Recovery Symposium, Tulsa, Oklahoma, 19–23 April.

Liauh, W.W., and Liu, T.W. 1984. A Capillary Viscometer for the Study of EOR Polymers. Paper SPE 12649 presented at the SPE/DOE Symposium on Enhanced Oil Recovery, Tulsa, Oklahoma, 15–18 April.

Manning, R.K., Pope, G.A., Lake, L.W., and Paul, G.W. 1983. A Technical Survey of Polymer Flooding Projects. Contract No. DOE/BC10327-19, US DOE, Washington, DC (September 1983).

Maerker, J.M. 1975. Shear Degradation of Partially Hydrolyzed Polyacrylamide Solutions. *SPEJ* **15**(4): 311–322, SPE 5101-PA.

Maerker, J.M. 1976. Mechanical Degradation of Partially Hydrolyzed Polyacrylamide Solutions in Unconsolidated Porous Media. *SPEJ* **16**(4): 172–174, SPE 5672-PA.

Masuda, Y., Tang. K-C., Mlyazawa, M., and Tanaka, S. 1992. 1D Simulation of Polymer Flooding Including the Viscoelastic Effect of Polymer Solution. *SPERE* **7**(2): 247–252, SPE 9499-PA.

Pang, S. and Sharma, M.M. 1997. A Model for Predicting Injectivity Decline in Water-Injection Wells. *SPEFE* **12**(3): 194–201, SPE 28489-PA.

Peterson, J.E. 1981. Coalinga Polymer Demonstration Project, Final Report July 1976-December 1980. Contract No. DOE/SAN/1556-5, US DOE, Washington DC (December 1981).

Pye, D.J. 1964. Improved Secondary Recovery by Control of Water Mobility. *JPT* **16**(8): 911–916, SPE 845-PA.

RP63, Recommended Practices for Evaluation of Polymers Used in Enhanced Oil Recovery. 1990. Washington, DC.: API.

Saripalli, K. P., Bryant, S. L., and Sharma, M.M. 1999. Role of Fracture Face and Formation Plugging in Injection Well Fracturing and Injectivity Decline. Paper SPE 52731 presented at the SPE/EPA Exploration and Production Environmental Conference, Austin, Texas, 28 February–3 March.

Schmidt, J.H., Friar, W.L., Bill, M.L., and Cooper, G.D. 1999. Large-Scale Injection of North Slope Drilling Cuttings. Paper SPE 52738 presented at the SPE/EPA Exploration and Production Environmental Conference, Austin, Texas, 28 February–3 March.

Seright, R.S., Maerker, J.M., and Holzwarth G. 1981. Mechanical Degradation of Polyacrylamides Induced by Flow Through Porous Media. *American Chemical Society Polymer Preprints*, **22**(August): 30–33.

Seright, R.S. 1983. The Effects of Mechanical Degradation and Viscoelastic Behavior on Injectivity of Polyacrylamide Solutions. *SPEJ* **23**(3): 475–485, SPE 9297-PA.

Seright, R.S. 1991. Effect of Rheology on Gel Placement. *SPERE* **6**(2): 212-218; *Trans.*, AIME, **291**.

Seright, R.S. 1993. Improved Techniques for Fluid Diversion in Oil Recovery. First Annual Report. Contract No. DE94000113. US DOE, Washington, DC (December 1993): 30–38.

Sharma, M.M., Pang, S., Wennberg, K.E., and Morgnthaler, L.N. 2000. Injectivity Decline in Water-Injection Wells: An Offshore Gulf of Mexico Case Study. *SPEPF* **15**(1): 6–13.

Smith, F.W. 1970. The Behavior of Partially Hydrolyzed Polyacrylamide Solutions in Porous Media. *JPT* **22**(2): 148–156. SPE 2422-PA.

Sorbie, K.S. 1991. *Polymer-Improved Oil Recovery*. Glasgow, Scotland, Blackie & Son, Ltd.: 115.

Van den Hoek, P.J. *et al.* 2008. Waterflooding under Dynamic Induced Fractures: Reservoir Management and Optimization of Fractured Waterfloods. Paper SPE 110379 presented at the SPE/DOE Improved Oil Recovery Symposium, Tulsa, Oklahoma, 19–23 April.

Wang, D., Han, P., Shao, Z., Weihong, H., and Seright, R.S. 2008. Sweep Improvement Options for the Daqing Oil Field. *SPEREE* **11**(1): 18–26. SPE 99441-MS.

Wreath, D., Pope, G.A., and Sepehrnoori, K. 1990. Dependence of Polymer Apparent Viscosity on the Permeable Media and Flow Conditions. *In Situ* **14**(3): 263-283.

Zhang, G. and Seright, R.S. 2007. Conformance and Mobility Control: Foams versus Polymers. Paper SPE 105907 presented at the SPE International Symposium on Oilfield Chemistry, Houston, Texas, 28 February–March 2.

SI Metric Conversion Factors

cp x 1.0*	E-03	= Pa·s
ft x 3.048*	E-01	= m
in. x 2.54*	E+00	= cm
md x 9.869 233	E-04	= μm^2
psi x 6.894 757	E+00	= kPa

*Conversion is exact